 doi:10.20944/preprints202201.0118.v1

Case-Crossover Spatial Lag Grid Differences Between Aerosol Optical Depth-$PM_{2.5}$ and Respiratory-Cardiovascular Emergency Department Visits and Inpatient Hospitalizations in Baltimore, Maryland, USA: Identification of Homogeneous Spatial Areas

John T. Braggio[1, 5,*], Eric S. Hall[2], Stephanie A. Weber[3, 6] and Amy K. Huff[4, 7]

[1]Maryland Department of Health, Baltimore, MD, 21201, USA
[2]U.S. Environmental Protection Agency, Research Triangle Park, NC, 27709, USA; hall.erics@epa.gov; ORCID ID: 0000-0002-0528-2014
[3]Battelle Memorial Institute, Columbus, OH, 43201, USA
[4]Battelle Memorial Institute, Arlington, VA, 22201, USA
[5]Mt. Diablo Analytical Solutions and Reporting Institute, LLC (Diablo Analytical Institute, DAI), 3474 Tice Creek Drive, Unit 7, Walnut Creek, CA 94595-3742, USA (permanent address); ORCID ID: 0000-0001-9129-7636
[6]Huntington National Bank, Columbus, OH 43215, USA; stephanieaweber@gmail.com (permanent address)
[7]IMSG at NOAA/NESDIS Center for Satellite Applications and Research, 5825 University Research Ct, Suite 3250, College Park, MD 20740, USA; amy.huff@noaa.gov (permanent address)
[*]Corresponding author (JTB): Email; johntbs@msn.com; Cell: (+1) 510-520-5149

Abstract: Optimal use of aerosol optical depth (AOD)-$PM_{2.5}$ fused surfaces in epidemiologic studies requires homogeneous temporal and spatial fused surfaces. No analytic method is currently available to evaluate the spatial dimension. The temporal case-crossover design was modified to assess the association between Community Multiscale Air Quality (CMAQ) lag grids and four respiratory-cardiovascular hospital events. The maximum number of adjacent lag grids with the exposure-health outcome association determined the size of the homogeneous spatial area. The largest homogeneous spatial area included 5 grids (720 km^2) and the smallest 2 grids (288 km^2). PMC and PMCK analyses of ED asthma, IP asthma, IP MI, and IP HF were significantly higher in rural grids without air monitors than in urban with air monitors at lag grids 0, 1, and 01. Grids without air monitors had higher AOD-$PM_{2.5}$ concentration levels, poverty percent, population density, and environmental hazards than grids with air monitors. ED asthma, IP MI, and HF PMCK ORs were significantly higher during the warm season than during the cold season at lag grids 0, 1, 01, and 04. The possibility of elevated fine PM and other demographic and environmental risk factors contributing to elevated respiratory-cardiovascular diseases in persons residing in rural areas was discussed.

Keywords: spatial heterogeneity, AOD-PM2.5, respiratory-cardiovascular, lag grids, urban-rural, season

1. Introduction

Published studies emphasize the detrimental effects of acute and chronic exposure to elevated ambient $PM_{2.5}$ concentration levels to respiratory-cardiovascular chronic disease morbidity and mortality [1-34]. Frequent, accurate, and timely measurements of ambient $PM_{2.5}$ concentration levels, obtained from on-the-ground air monitors, are

essential for protecting human health and decreasing respiratory-cardiovascular morbidity and mortality [8, 17, 19, 21, 28, 29, 35-42]. There are challenges in using ambient $PM_{2.5}$ air monitors, especially those maintained by the U.S. Environmental Protection Agency (EPA) Air Quality System (AQS) [38] in epidemiologic studies [3, 32]. The majority of these $PM_{2.5}$ filter-based monitors measure $PM_{2.5}$ concentration levels every three or six days in urban areas with higher population density [3, 32, 38]. Few studies have evaluated differences between urban-rural areas [16, 43-48]. Increasing the number of stationary $PM_{2.5}$ air monitors in rural areas would provide accurate readings of fine PM concentration levels and decrease spatial heterogeneity. Epidemiologic studies could use $PM_{2.5}$ readings made in rural areas to determine fine PM's short- and long-term contribution to the occurrence of respiratory-cardiovascular hospital events [3, 23, 49]. Unfortunately, this type of enhancement to the AQS air monitoring network would be expensive to implement and maintain [38, 50-52].

An alternative would be to utilize remote sensing methodology. Increased emphasis on using remote sensing would result in obtaining cost-effective readings of $PM_{2.5}$ concentration levels in urban and rural areas [3, 6, 9, 13, 16, 20, 22, 24, 30, 32, 46-48, 51-78]. Different investigators have combined satellite AOD readings with $PM_{2.5}$ air monitor measurements by utilizing Hierarchical Bayesian Model (HBM) or other statistical procedures to attain continuous (homogeneous) temporal-spatial aerosol concentration level fused surfaces that represent ambient $PM_{2.5}$ concentration levels in urban areas that have air monitors and in rural areas that do not have air monitors [3, 6, 9, 13-16, 20, 22, 30, 32, 48, 51, 52, 55, 59-61, 64-66, 68-74, 77, 79-82].

Urban and rural areas also differ on residents' demographics. Urban areas have more poverty, greater population density, and more non-Hispanic non-white residents than rural areas [3, 37, 43]. Higher population density was an important factor in the placement of on-the-ground air monitors in the Baltimore study area. To what extent ambient $PM_{2.5}$ concentration levels influenced that decision is unknown. In this context, for the Baltimore study area, Braggio and associates' [3] use of four AOD-$PM_{2.5}$ and baseline PMB fused surfaces provided support for the placement of air monitors in urban 12 km^2 CMAQ grids with air monitors and not in rural grids without air monitors [83]. Urban grids had elevated fine PM levels and higher population density than rural grids. Three of the four AOD-$PM_{2.5}$ and PMB fused surfaces had significantly higher 2004-2006 mean $PM_{2.5}$ concentration levels in the 15 urban grids with air monitors compared to the 84 rural grids without air monitors. In another Baltimore study area publication Braggio and colleagues [84] reported similar AOD-$PM_{2.5}$ and respiratory-cardiovascular relationships (i.e., concentration-response functions) in urban grids with air monitors and in rural grids without air monitors.

Numerous publications have emphasized the importance of describing the temporal and spatial attributes of $PM_{2.5}$ concentration levels measured by ambient air monitors [26, 33, 37, 49, 71, 85-88] and by AOD-$PM_{2.5}$ in areas with and without air monitors [3, 15, 20, 22, 48, 52, 57-59, 61, 63, 67, 71, 78, 80, 81, 84, 89-93]. Our interdisciplinary research team, with members from the Battelle Memorial Institute, the U.S. Centers for Disease Control and Prevention (CDC), funded Environmental Public Health Tracking (EPHT) programs at the Maryland Department of Health and the New York State Department of Health, and the EPA initially developed the baseline PMB and subsequently assembled the four experimental AOD-$PM_{2.5}$ concentration level fused surfaces, by statistically combining $PM_{2.5}$ monitor readings with National Aeronautics and Space Administration (NASA) AOD data from the MODerate Resolution Imaging Spectroradiometer (MODIS) instrument on the Aqua and Terra satellites and CMAQ $PM_{2.5}$ model estimates [94-96] for the New York City [32] and Baltimore [3, 84] study areas. The New York City study area utilized the four AOD-$PM_{2.5}$ concentration level fused surfaces and PMB to determine the temporal contribution of these five fused surfaces to emergency department (ED) asthma visits, inpatient (IP) asthma, IP myocardial infarction (MI), and IP heart failure (HF) hospitalizations [32]. In the Baltimore study area, with significantly higher three-year mean

fine PM ($PM_{2.5}$) concentration levels for the four AOD-$PM_{2.5}$ and baseline PMB fused surfaces than in the New York City study area, we found two AOD-$PM_{2.5}$ fused surfaces, PMC and PMCK, that reliably and accurately contributed to increased respiratory-cardiovascular ED visits and IP hospitalizations in urban grids with air monitors and in rural grids without air monitors, at lag days 0, 1 and 01 [3, 84].

The 99 12 km^2 CMAQ grids which define the Baltimore study area, are temporally and spatially heterogeneous on resident demographics, placement of on-the-ground air monitors and ambient $PM_{2.5}$ concentration levels. The Baltimore study area's spatial heterogeneity consisted of differences between urban grids with air monitors and rural grids without air monitors [3, 84]. Urban grids with air monitors represent a more spatially homogeneous area given the *a priori* criteria used to select those areas to install air monitors. The 15 urban grids with air monitors in the Baltimore study area share similar attributes that include higher poverty, greater population density and elevated ambient $PM_{2.5}$ concentration levels. Since the number of rural grids without air monitors outnumber the number of urban grids with air monitors by 560%, there could be a smaller group of rural grids that resembles the urban grids by also demonstrating higher poverty, population density and ambient $PM_{2.5}$ concentration levels. Residents in these higher risk homogeneous rural grids should resemble urban grids by displaying a similar association between elevated fine PM concentration levels and increases in respiratory-cardiovascular ED visits and IP hospitalizations.

To identify homogenous spatial areas that demonstrate a similar relationship between elevated AOD-$PM_{2.5}$ concentration levels and increased respiratory-cardiovascular ED visits or IP hospitalizations we modified the temporal (lag day) case-crossover design to identify spatial homogeneous grids. In the lag day case-crossover design all exposure-health outcome assessments occur in the patients' grid of residence. The date when the patient received medical care is the index day or lag day 0: The day preceding the index day is lag day 1. Two-four days before the index day are identified as lag days 2-4, respectively. The spatial (lag grid) case-crossover design evaluates the association between exposure and outcome on the same day but in different grids. The patients' grid of residence is the index grid. It has a lag grid value of 0. The grid that is next to and spatially precedes the index grid is lag grid 1. Two to four grids that spatially precede the index grid are referred to as lag grids 2-4, respectively. The lag day and lag grid case-crossover formatted linked exposure-health outcome data files were analyzed using conditional logistic regression (CLR). CLR analyses compute odds ratios (ORs) for lag days and lag grids. Significant ORs identify lag days or lag grids with elevated AOD-$PM_{2.5}$ concentration levels and increased respiratory-cardiovascular ED visits or IP hospitalizations.

By implementing the spatial lag grid case-crossover design it will be possible to identify homogeneous spatial areas that share the same relationship between AOD-$PM_{2.5}$ and PMB fused surface concentration levels and increased respiratory-cardiovascular ED visits or IP hospitalizations in the entire Baltimore study area and in urban grids with air monitors and in rural grids without air monitors. The first objective of this study will be to determine the size of the homogeneous spatial area, measured as multiples of CMAQ 12 km^2 grids, for each of the four experimental AOD-$PM_{2.5}$ and PMB fused surfaces. Homogeneous spatial areas are those with significant lag grid ORs that demonstrate a similar exposure-health outcome association. Another aim will be to determine if AOD-$PM_{2.5}$ and PMB concentration levels differ between urban grids with air monitors and rural grids without air monitors. This analysis will determine if rural grids without air monitors have higher AOD-$PM_{2.5}$ and PMB concentration levels and increased respiratory-cardiovascular ED visits or IP hospitalizations than urban grids with air monitors. A third aim will be to evaluate warm-cold season differences [3, 7, 8, 10, 13, 18, 20, 23, 28, 31, 32, 41, 49, 51, 55, 56, 67, 77, 89, 97-99] in in the entire Baltimore study area and in grids with and without air monitors. In CLR analyses of warm-cold season differences this study will look more closely at the relationship between ambient temperature and AOD-$PM_{2.5}$

Preprints (www.preprints.org) | NOT PEER-REVIEWED | Posted: 10 January 2022 doi:10.20944/preprints202201.0118.v1

and PMB fused surface concentration levels after controlling for the confounding effects of apparent temperature (AT). Separate warm-cold season analyses will also evaluate the relationship between ambient temperature and AOD-$PM_{2.5}$ concentration levels for the year and each season in the Baltimore study area and in grids with and without air monitors.

2. Materials and Methods

This study implemented the lag grid case-crossover design and utilized the same four experimental AOD-$PM_{2.5}$ and PMB concentration level fused surfaces and the same four respiratory-cardiovascular chronic disease groups that were previously used in the lag day case-crossover studies completed for the Baltimore [3, 84] and New York City [32] study areas. This section will include lag grid case-crossover study details. Other information about the lag day analyses are in earlier publications describing the Baltimore [3, 84] and New York City [32] study areas.

Baltimore Study Area

Table 1 displays the 11 (South [S] to North [N]) by 9 (West [W] to East [E]) 99 12 km^2 CMAQ grids – these grids defined the Baltimore study area [3, 84]. The 17 federal reference method (FRM) ambient $PM_{2.5}$ air monitors, which were operational in 2004-2006,

Table 1: Bidirectional Spatial Lag Grid Case-Crossover Analyses for the 99 12 km^2 CMAQ Grids With (Red) and Without (Clear) Ambient $PM_{2.5}$ Air Monitors in the Baltimore Study Area[a-c].

(11,1)				N (11, 5)				(11, 9)
					(8, 6/B)		**(8, 8/H)**	
				(7, 5/BC)	**(7, 6/BC)**	**(7, 7/B)**		
W (6, 1)					**(6, 6/BC)**	**(6, 7/BC)**		E (6, 9)
					(5, 6/AA)	**(5, 7/AA)**		
		(4, 3/M)		**(4, 5/PJ)**	**(4, 6/AA)**			
				(3, 5/PJ)		**(3, 7/AA)**		
					(2, 6/PJ)			
(1, 1)				S (1, 5)				(1, 9)

[a]CMAQ grid coordinates, shown in black hue, are 1-11 (South [S] to North [N]) rows and 1-9 (West [W] to East [E]) columns. [b]Grid coordinates, displayed in a red hue and in bold font, had one or more ambient FRM $PM_{2.5}$ air monitors. One urban grid (**R_6, C_6**) in Baltimore City had three $PM_{2.5}$ air monitors. The other 14 urban grids with air monitors had one ambient $PM_{2.5}$ air monitor per grid. [c]These are the county/city abbreviations used in each CMAQ grid: AA = Anne Arundel County; B = Baltimore County; BC = Baltimore City; H = Hartford County; M = Montgomery County; PJ = Prince George's County.

are in the 15 grids with air monitors. The grids with ambient air monitors are identified with row-column grid coordinates, city/county abbreviations and are displayed in red hue in Table 1. There were 6 air monitors in BC, 4 in AA, 3 in PJ, 2 in B, and 1 each in M and in H Counties.

ED and IP Hospitalizations

The assessment included the four respiratory-cardiovascular chronic disease hospitalization end points. The 4 health data files consisted of all 2004-2006 ED visits and IP hospitalizations in Maryland, reported by State statute, to the Maryland Health Services Cost Review Commission [HSCRC, 100]. Individual HSCRC electronic patient records did not include patient names, social security numbers, and residential addresses. However, each electronic patient record had temporal information about the ED visits and IP hospitalizations (year [2004-2006], quarter [winter, spring, summer, fall], day of the

week [Sunday through Saturday], date of birth, gender, race, health insurance, spatial location for the residential address, five-digit U.S. Postal Service (USPS) residential Zone Improvement Plan (ZIP) code [101], and one primary and multiple secondary diagnostic fields, with International Classification of Diseases, Ninth Revision, Clinical Modification (ICD-9-CM) billing codes [102]. ICD-9-CM codes permitted the identification of electronic patient records with ED asthma visits and IP asthma (493), IP MI (410), and IP HF (428) hospitalizations in the primary diagnosis field. In addition, ICD-9-CM codes identified which electronic patient records had one or more of the three comorbid chronic diseases of atherosclerosis (414, 440), diabetes mellitus (250), and hypertension (401). The study's protocol, including the proposed data analyses, were approved by the Maryland Department of Health Institutional Review Board (IRB) [103] and the Maryland Health Services Cost Review Commission [100]. The MDH IRB concluded that since this study only utilized administrative hospital data, and because there was no contact with patients, it was approved through an exempted review.

Controls

There were three controls for each case. While the electronic patient records for the controls were the same as those for the cases, the cases had a different quarterly $PM_{2.5}$ exposure value than the quarterly $PM_{2.5}$ exposure values assigned to the controls. Three different monthly control exposure sampling strategies were utilized: first control was assigned the mean of the $PM_{2.5}$ concentration levels for January [winter], April [spring], July [summer] and October [fall]; second control included $PM_{2.5}$ concentration levels for February [winter], May [spring], August [summer] and November [fall]; and, third control comprised $PM_{2.5}$ concentration levels for March [spring], June [summer], September [fall] and December [winter].

Case-Control Strata

Each stratum included one case and three controls [3, 32, 84]. There were four different quarterly strata, each including a case with a different quarterly mean $PM_{2.5}$ concentration level exposure value. Three controls were in each of the four quarterly strata but, as stated above, they differed from the cases on the assigned mean quarterly $PM_{2.5}$ concentration level values [104]. The case and control means of the monthly ranks were used to confirm that the Braggio and associates [3, 84] studies utilized a bidirectional temporal lag day case-crossover design [105]. Months were ordered in ascending order, from January (1) through December (12), and then the monthly ordinal ranks of 1-12 were assigned to each month, respectively. Cases with quarterly exposure values had mean monthly ranks of 2.0 for winter, 5.0 for spring, 8.0 for summer, and 11.0 for fall. The mean monthly ranks for the three controls were 5.5 (1 = January; 4 = April; 7 = July; 10 = October) for first control, 6.5 (2 = February; 5 = May; 8 = August; 11 = November) for the second and 7.5 (3 = March; 6 = June; 9 = September; 12 = December) for the third. For the first and second strata, mean quarterly ranks for the three controls were higher than the mean quarterly ranks for the two cases. In the last two strata, the mean quarterly ranks for the three controls were lower than the mean quarterly ranks for the two cases. Each case and the three associated controls were matched on age, gender, race, health insurance, residential ZIP code, year, and day of the week. $PM_{2.5}$ concentration levels and effect modifiers varied temporally by year (3), quarter (4), day of the week (7), and spatially by CMAQ grid (99), thereby resulting in 8316 different possible variable combination values for the four AOD-$PM_{2.5}$ and PMB fused surfaces. There were fewer CMAQ grids with fused surface concentration level values and health data: 15 with air monitors and 57 without air monitors, for a total of 72 CMAQ grids with heath data. Warm-cold season differences were preserved for subsequent analyses by using this bidirectional lag grid case-crossover design.

Confounders

The comorbid health conditions included atherosclerosis [3, 39, 84], hypertension [3, 32, 39, 84], and diabetes [3, 10, 32, 84, 106-108]. Other confounders were apparent-temperature (AT, AT^2; [3, 32, 39, 84, 109, 110]) and pollen [3, 7, 35, 36, 84, 111-115]. Major holidays (and the day after) were coded as dummy variables (1 = holiday or the day after, 0 = no holiday) in each annual ED visit and IP hospitalization file [3, 32, 84, 116]. Dummy variables were used to code snowstorms (1 = yes; 0 = no) in each of the three annual files [3, 32, 84, 117].

Effect Modifiers

Poverty [3, 35-37, 44, 84, 118-120] and population density [3, 84] were two geographic-based demographic variables that came from the U.S. Census Bureau [121] and the Maryland Department of Planning, Maryland Data Center [122]. Maryland Zip Code Tabulation Area (ZCTA) spatial polygons for poverty and persons per square mile were obtained from the U.S. Census Bureau website [121].

AOD-$PM_{2.5}$ and PMB Fused Surfaces

The same four experimental AOD-$PM_{2.5}$ and PMB concentration level fused surfaces, previously described in detail in earlier publications [3, 32, 84] were used in this lag grid case-crossover data analysis study. The MODIS instrument on the two orbiting satellites, Terra and Aqua, obtained daily readings, the first in the morning (10:30 AM) and the other in the afternoon (1:30 PM), local time. The AOD measurement column was continuous from each satellite's trajectory in space to the earth's surface. $PM_{2.5}$ particles within the AOD column changed the light refraction properties, thereby making it possible to obtain AOD unitless measurements. Thus, the AOD readings represented proxies for ambient $PM_{2.5}$ concentration levels. The previously established relationship between the AOD unitless value and the ambient $PM_{2.5}$ concentration level was used to assign a corresponding $PM_{2.5}$ concentration level value to each AOD unitless value. Implementing this algorithm resulted in a continuous space-time AOD-$PM_{2.5}$ fused surface [3, 32, 84, 94-96].

The updated HBM permitted the fusing of two or three different input surfaces with (not-Kriged) or without (Kriged) missing AOD-$PM_{2.5}$ concentration level readings. PMC represented the inclusion of ambient $PM_{2.5}$ monitor measurements with AOD-$PM_{2.5}$ concentrations levels. Satellite recording failure or the presence of cloud cover interfered with obtaining unitless AOD column readings, thereby resulting in missing data values. To minimize the loss of daily AOD readings, a second AOD-$PM_{2.5}$ fused surface was Kriged, resulting in the PMCK fused surface – the HBM fusion of monitor $PM_{2.5}$ with Kriged PMC concentration levels. For the two remaining AOD-$PM_{2.5}$ fused surfaces, the HBM was used to combine PMC (not Kriged) or PMCK (Kriged) with monitor $PM_{2.5}$ readings and CMAQ $PM_{2.5}$ model estimates to produce PMCQ (not-Kriged PMC) and PMCKQ (Kriged PMCK), respectively. Using the HBM, it was also possible to make PMB – the baseline fused surface, by combining $PM_{2.5}$ monitor readings with CMAQ $PM_{2.5}$ model estimates. The four experimental AOD-$PM_{2.5}$ and PMB fused surfaces were displayed within the EPA CMAQ grid system by overlying the NASA native 10 km^2 AOD grid onto the EPA native 12 km^2 CMAQ grid.

File Linkage

The use of a previously developed polygon correspondence file minimized the spatial mismatch between the various irregular-shaped polygon files [123]. The polygon correspondence file made it possible to assign each USPS ZIP code polygon (health outcome), U.S. Census Bureau ZCTA polygon (poverty percent and population density), and CMAQ 12 km^2 grid template (four experimental AOD-$PM_{2.5}$ and PMB concentration level fused surfaces) to one CMAQ grid [3, 84]. Assembling the polygon correspondence file necessitated completing these steps: 1) Obtaining latitude-longitude centroid coordinates for each ZIP code and ZCTA polygons [83, 121, 122]. 2) Using a geographic information system (GIS) to assign each residential ZIP code polygon or ZCTA polygon to one CMAQ 12 km^2 grid, based on the spatial location of each latitude-longitude centroid coordinate

of each polygon within a specific CMAQ grid [124]. By using the correspondence file, it was possible to implement the CMAQ 12 km^2 grid system as the standardized spatial polygon template for this data analysis study [3, 83, 84, 123, 124].

Each of the four linked AOD-$PM_{2.5}$ files (one for ED asthma, a second for IP asthma, a third for IP MI, and a fourth for IP HF) was sorted on the spatial grid coordinates first and temporal values next. The sorting sequence for the Baltimore study area was columns first then rows, followed by the temporal variables of weekday, quarter, and year [3, 84]. But, for this spatial lag grid analysis study, only the sorting sequences of columns and rows were implemented because they were of primary importance in this lag grid case-crossover study.

Bidirectional Case-Crossover Spatial Lag Grid Analyses

The lag grid case-crossover analysis resembled the lag day case-crossover analysis, except that the spatial analysis evaluated lag grids, including the index grid, which always had a value of 0 (including all lag grids of 0-4, 01, 24, and 04), while the temporal analysis assessed lag days preceding the index day, which always had a value of 0 (including all lag days of 0-4, 01, 24 and 04). In the New York City [32] and Baltimore [3, 84] studies, we utilized a bidirectional lag day case-crossover design to determine if there were differences due to asthma ED visits, and IP asthma, IP MI, and IP HF hospitalizations among the individual lag days (0-4) and summary lag days (01, 24, and 04) [3]. The lag day analysis determined if ambient $PM_{2.5}$ concentration levels, evaluated by the four experimental AOD-$PM_{2.5}$ and PMB concentration level fused surfaces, differentially contributed to the subsequent occurrence of one or more respiratory-cardiovascular ED visits or IP hospitalizations. In the lag day analysis, all outcomes were evaluated on different days but in the same grid. In the lag grid analysis, all outcomes were evaluated in different grids but on the same day.

The overall objective of the lag grid case-crossover assessment was to identify the number of 12 km-wide grid units from the index grid that demonstrated the same association between each of the four AOD-$PM_{2.5}$ and PMB fused surface concentration levels and each of the four respiratory-cardiovascular hospital outcomes, ED visits or IP hospitalizations.

Table 2: Three Examples of Bidirectional Spatial Lag Grid Case-Crossover Analyses, by Ambient $PM_{2.5}$ Air Monitor Status: No Monitors, Monitors, and Both Monitor Grid Conditions Combined. Grids with Monitors are Shown in Red Hue and in Bold Font.

Grid Monitor Examples[a]	Spatial Lag Grid Analyses[b]							
	0	1	2	3	4	01	24	04
No Monitors								
Rows (S to N)	**R_9**	**R_9**	**R_9**	**R_9**	**R_9**	**R_9**	**R_9**	**R_9**
Columns (W to E)	**C_7**	**C_6**	**C_5**	**C_4**	**C_3**	**C_{6-7}**	**C_{3-5}**	**C_{3-7}**
Monitors								
Rows (S to N)	**R_6**	**R_6**	**R_7**	**R_7**	**R_7**	**R_6**	**R_7**	**$R_{6,7}$**
Columns (W to E)	**C_7**	**C_6**	**C_7**	**C_6**	**C_5**	**C_{6-7}**	**C_{5-7}**	**$C_{6-7, 5-7}$**
Both – All Grids								
Rows (S to N)	**R_4**	**R_4**	**R_4**	**R_4**	**R_4**	**R_4**	**R_4**	**R_4**
Columns (W to E)	**C_7**	**C_6**	**C_5**	**C_4**	**C_3**	**C_{7-6}**	**C_{5-3}**	**C_{7-3}**

[a]Row (South [S] to North [N]) and column (West [W] to East [E]) grid coordinates for the Baltimore study area are shown here. The sorting sequence was the column variable (1 to 9) first and the row variable (1 to 11) second. [b]Lag grid 0 is the index grid. Lag grid 1 refers to the grid that preceded the index grid by 1 grid distance, 12 km. Lag grids 2 through 4 preceded the index grid by 2 to 4 grids, 24 km to 48 km, respectively. Lag grid 01 represents the mean of values for grids 0 and 1. Lag grid 24 refers to the mean for grids 2-4. Lag grid 04 represents the mean for lag grids 0-4.

The implementation of the lag grid case-crossover analysis is described in the three examples shown in Table 2. The first illustration is for grids without monitors, top of the table. The Spatial Lag Grid Analyses column displays lag grid values, both individual (0-4) and summary measures (01, 24, 04). The grid location for the individual grids with monitors is shown in bold red font for grids with air monitors and bold black font for grids without air monitors. The index grid location for the no monitor example is Row = 9 and Column = 7 (R_9, C_7). This index grid has a lag grid value of 0. Moving from the far-right side of the table (East) to the left side of the table (West), the grid adjacent to and immediately to the left of the index grid has a lag grid value of 1, and its grid location is R_9, C_6. The next three lag grids, with lag grid values 2-4, have sequential grid locations: R_9, C_5; R_9, C_4; and R_9, C_3, respectively. Summary lag grids 01, 24, and 04 were obtained by computing means for individual lag grid values. To illustrate, the summary lag grid 01 represents the mean for lag grids 0 and 1. Lag grid 24 includes the mean for lag grids 2-4. Lag grid 04 refers to the mean for lag grids 0-4.

The second example, shown in the middle of the table, is for lag grids with air monitors. Here, the index grid location is R_6, C_7. Again, the index grid has a lag grid value of 0. The first two lag grids with monitors are in the 6th row, while the next three lag grids with monitors are in the 7th row. Notice that column location decreases by 1 as the lag grid value increases by 1.

The third example, at the bottom of Table 2, is for both monitor grid conditions combined. The index grid location is R_4, C_7. All five individual lag grids, with lag grid values of 0-4, are in the 4th row. Three of the five lag grids, 1, 2 and 4, include air monitors. The other two lag grids, 0 and 3, include grids without monitors.

Considering the spatial lag grid analysis descriptions summarized in Tables 1 and 2, it is possible to demonstrate that the three types of lag grid analyses presented above represent the inclusion of lag grids that either precede or follow the index grid, based on the index grid column location. Each complete lag grid sequence always includes five individual lag grid values, the index grid, and four additional lag grids. The four lag grids are selected from 1-4 lag grids that always precede the index grid. This prior selection of lag grids, relative to the location of the index grid, occurs for columns 9 E to 5 W. But, for the remaining four columns, 4 E to 1 W, the selection of the four preceding lag grids, relative to the location of the index grid, will invariably include 1-4 grids that always follow the index grid. To illustrate, when the index grid has a column location value of 4, the selection of the four preceding grids will result in the inclusion of column 3 for lag grid 1, column 2 for lag grid 2, column 1 for lag grid 3, and column 9, in one row above, for lag grid 4. When the index grid is in column 3, two grids precede the index grid, and two grids follow the index grid. The index grid for column 2 includes 1 grid that precedes the index grid and three grids that follow the index grid. For the fourth lag grid, when the index grid is in column 1, all four lag grids follow the index grid and are in the above row.

These are the results for all grids that preceded or followed the index grid: For grids with monitors, 62.0% of the grids had the same column value or a lower column value (preceded) than the index grids, and 38% of the grids had column values that were larger (followed) than the column values of the index grids. For grids without monitors, 69.3% preceded the index grids, and 30.7% followed the index grids. The combined no monitor grids with monitor grids included 68.4% of the grids preceded the index grids, and 31.6% followed the index grids. To summarize, these results support the conclusion that this spatial lag grid case-crossover design included lag grids that preceded or followed the index grid; thus, this outcome demonstrates that this study implemented a bidirectional lag grid case-crossover design [3, 32, 84, 105].

Statistical Analyses

The four linked fine PM exposure-health outcome files, one each for ED asthma, IP asthma, IP MI, and IP HF were analyzed using CLR statistical software included in the

SAS (Statistical Analysis System)/STAT proportional hazards ratio (PHREG) Procedure, version 14.3, along with Base SAS version 9.4 [3, 32, 84, 125-129]. PHREG performs CLR analyses on survival data, based on the Cox Proportional Hazards model, by quantifying the effects of explanatory variables on survival times. The Chi Square test evaluated group differences between categorical variables, such as case-control status, gender, and race [127]. Assessment of continuous variables, such as poverty percent and population density (converted to L_{10} values before analysis), involved comparing a case group mean to a control group mean and its associated 95% Confidence Interval (CI). Means and 95% CIs were obtained from Proc Means in Base SAS [127]. If the case mean was below or above the 95% CI lower or upper limits of the control group mean, this outcome was significantly different at $p \leq 0.05$ [125]. But, if the case mean was within the 95% CI lower and upper limits of the control mean, this outcome was not significant, $p > 0.05$.

Variable Selection

The CLR runs consisted of a $PM_{2.5}$ fused surface (PMB, PMC, PMCK, PMCQ, PMCKQ) and one respiratory-cardiovascular endpoint (ED asthma, IP asthma, IP MI, or IP HF). CLR runs evaluated individual lag grids 0-4 and summary lag grids 01, 24, and 04. The base CLR analysis controlled for these confounders ([apparent temperature, AT – at each grid lag; AT^2 – at lag grids 0, 1, 01, and 04; pollen, snowstorms, major holidays [3, 32, 84, 113, 114, 117]. Four separate CLR runs evaluated effect modifiers: 1) diabetes mellitus, hypertension, atherosclerosis; 2) gender, age, race; 3) health insurance coverage, poverty percent, population density, and 4) season. An effect modifier was included in subsequent analyses if the initial CLR OR had a probability value of $p \leq 0.09$ [3, 84].

Final CLR Runs

Final CLR runs included the base model, effect modifiers for lag grids 0-4, and summary lag grids 01, 24, and 04. The three grid monitor conditions included grids without a monitor (No), grids with at least one monitor (Yes), and grids with or without monitors (Both). The null hypothesis was rejected if $p \leq 0.05$. The additional use of the Akaike Information Criterion (AIC) permitted the selection of CLR outcomes with lower values, thereby representing a better parameter fit [125, 126]. Follow-up analyses evaluated the contribution of monitor (No, Yes) and season (Warm, Cold) in lag grids 0-4, 01, 24, and 04 [3].

3. Results

CLR runs evaluated the contribution of the four AOD-$PM_{2.5}$ and PMB fused surfaces to the four health outcomes (ED asthma, IP asthma, IP MI, and IP HF) in grids (with air monitors, without air monitors, and both) at lag grid values of 0-4, 01, 24, and 04. Differences between experimental AOD-$PM_{2.5}$ and PMB concentration level fused surfaces

Table 3: Three-Year Mean (95% CIs) $PM_{2.5}$ Concentration Levels, Totals (%) Below, Within and Above the Mean and 95% CIs for PMB and the four Experimental AOD-$PM_{2.5}$ Concentration Level Fused Surfaces and Demographics, by Monitor Status.

Variables	CMAQ Grids with Ambient $PM_{2.5}$ Air Monitors[a-c]		
Fused Surfaces	Both	Yes	No
PMB[†]	14.19 (14.13-14.26)[†]	14.60 (14.44-4.76)	14.12 (14.05-14.19)
Below	38 (38.38)[‡]	4 (26.67)[†]	34 (40.48)[‡]
Within	6 (6.06)	1 (6.67)	5 (5.95)
Above	55 (55.56)	10 (66.67)	45 (53.57)
PMC[†]	13.66 (13.60-3.72)[†]	13.90 (13.73-4.06)	13.62 (13.55-13.68)
Below	52 (52.53)[‡]	7 (46.67)	45 (53.57)[‡]
Within	17 (17.17)	1 (6.67)	16 (19.05)
Above	30 (30.30)	7 (46.67)	23 (27.38)

 doi:10.20944/preprints202201.0118.v1

PMCK	14.38 (14.31-4.44)†	14.27 (14.10-14.44)	14.39 (14.32-14.47)
Below	36 (36.36)‡	8 (53.33)	28 (33.33)‡
Within	18 (18.18)	2 (13.33)	16 (19.05)
Above	45 (45.45)	5 (33.33)	40 (47.62)
PMCQ†	13.79 (13.73-3.85)†	14.28 (14.12-4.43)	13.71 (13.64-13.77)
Below	39 (39.39)‡	3 (20.00)†	36 (42.86)‡
Within	7 (7.07)	2 (13.33)	5 (5.95)
Above	53 (53.54)	10 (66.67)	43 (51.19)
PMCKQ†	13.91 (13.85-3.97)†	14.24 (14.09-4.40)	13.85 (13.79-13.92)
Below	38 (38.38)‡	4 (26.67)	34 (40.48)‡
Within	9 (9.09)	2 (13.33)	7 (8.33)
Above	52 (52.53)	9 (60.00)	43 (51.19)
Demographics			
Poverty Percent†	8.27 (7.84-8.69)	15.44 (14.13-16.76)	6.41 (6.01-6.80)
Below‡	51 (75.00)‡	7 (50.00)	44 (81.48)‡
Within	2 (2.94)	0 (0.00)	2 (3.70)
Above	15 (22.06)	7 (50.00)	8 (14.81)
Population Density	2.77 (2.75-2.78)	3.16 (3.12-3.21)	2.66 (2.65-2.68)
Below‡	36 (52.94)‡	3 (21.43)	33 (61.11)‡
Within	2 (2.94)	0 (0.00)	2 (3.70)
Above	30 (44.12)	11 (78.57)	19 (35.19)

[a]99 CMAQ 12 km^2 grids in the Baltimore study area. [b]Number (%) displayed in each cell. [c]Significance based on mean and 95% CI differences for continuous variables, and Chi Square (exact) for categorical variables: Monitor versus no monitor or both monitor groups combined for Below, Within or Above groups: †$p \leq 0.05$, ‡$p \leq 0.01$.

and demographics for all conditions are displayed in Table 3. The categorical analyses of $PM_{2.5}$ concentration levels that were Below, Within, or Above the three-year fused surface mean's 95% CIs for each of the three grid conditions showed significant heterogeneity in all grids (Both), and in grids with (Yes), and without (No) air monitors. PMCK concentration level was significantly higher than PMB concentration level in the Both and No monitor grid groups, and significantly lower in grids with monitors (all p's≤ 0.05). PMC, PMCQ, and PMCKQ concentration levels were significantly lower than PMB concentration levels in all three monitor grid conditions (all p's≤ 0.05). Also, in all grids, PMB and the two AOD-$PM_{2.5}$ fused surfaces that included CMAQ $PM_{2.5}$ model estimates, PMCQ and PMCKQ, resembled each other in number (52-55) and percentage (52%-56%) of grids with $PM_{2.5}$ three-year concentration level mean values in the Above category. For the other two AOD-$PM_{2.5}$ fused surfaces, PMC and PMCK, the number and percentage (30, 30% and 45, 45%, respectively) of grids with mean $PM_{2.5}$ concentration levels in the Above category in all grids were lower than PMB (55, 56%). Monitor versus no monitor comparisons showed that $PM_{2.5}$ concentration levels for PMB and three of the four AOD-$PM_{2.5}$ fused surfaces – PMC, PMCQ, and PMCKQ – were significantly higher in grids with air monitors than in grids without air monitors (all p's≤ 0.05). Only PMCK had $PM_{2.5}$ concentration levels that were not significantly different in grids with (14.27 μg/m^3) and without (14.39 μg/m^3) air monitors, both p's>0.05.

As seen at the bottom of Table 3, categorical analyses yielded new information about differences in grids with and without air monitors, which were not evident in the continuous measures for poverty percent and population density. Results for continuous measures supported the anticipated outcome of higher poverty percent and elevated population density in grids with air monitors compared to grids without air monitors (both p's≤ 0.05). For the demographic measures of poverty percent and population density, evaluated as categorical variables, there were more grids in the Above category in grids

 doi:10.20944/preprints202201.0118.v1

without monitors (8 [15%] for poverty percent and 19 [35%] for population density) than in grids with monitors (7 [50%] for poverty percent and 11 [79%] for population density).

Table 4 shows totals and percentages for the four respiratory-cardiovascular ED visit and IP hospitalization groups stratified on case-control status and patients' race. As seen in the Both column, second from left, ED asthma had the most observations (cases and

Table 4: Demographics for Respiratory-Cardiovascular Chronic Disease Cases and Controls, and Patients' Race in the Baltimore Study Area Lag Grid Analyses, by Monitor Status.

Variables	CMAQ Grids with Ambient $PM_{2.5}$ Monitors[a-b]		
	Both	Yes	No
ED Asthma	47256 (100.00)	20815 (44.05)	26441 (55.95)
Cases	11723 (24.81)	5152 (10.90)	6571 (13.91)
Controls	35533 (75.19)	15663 (33.14)	19870 (42.05)
Black‡	22696 (48.24)	11844 (25.17)	10852 (23.06)
Other	3060 (6.50)	785 (1.67)	2275 (4.84)
White	21294 (45.26)	8082 (17.18)	13212 (28.08)
IP Asthma	13515 (100.00)	5672 (41.97)	7843 (58.03)
Cases	3376 (24.98)	1417 (10.48)	1959 (14.50)
Controls	10139 (75.02)	4255 (31.48)	5884 (43.54)
Black‡	4510 (33.43)	2358 (17.48)	2152 (15.95)
Other	669 (4.96)	179 (1.33)	490 (3.63)
White	8312 (61.61)	3119 (23.12)	5193 (38.49)
IP MI	19021 (100.00)	7185 (37.42)	12016 (62.58)
Cases	4790 (24.95)	1784 (9.29)	3006 (15.66)
Controls	14411 (75.05)	5401 (28.13)	9010 (46.92)
Black‡	2456 (13.28)	1183 (6.17)	1363 (7.11)
Other	848 (4.42)	180 (0.94)	668 (3.48)
White	15780 (82.30)	5811 (30.31)	9969 (51.99)
IP HF	27518 (100.0)	11834 (43.00)	15684 (57.00)
Cases	6826 (24.81)	2928 (10.64)	3898 (14.17)
Controls	20692 (75.19)	8906 (32.36)	11786 (42.83)
Black‡	7029 (25.57)	3463 (12.60)	3566 (12.97)
Other	793 (2.88)	285 (1.04)	508 (1.85)
White	19672 (71.55)	8078 (29.38)	11594 (42.17)

[a]Total grids with health data = 72: 15 with monitors and 57 without monitors.
[b]Number (%): ‡$p \leq 0.01$, Chi-Square, no monitor versus monitor.

controls combined, 47256), IP Asthma the fewest (13515), with intermediate totals for IP MI (19201) and IP HF (27518). Totals and percentages for each of the four health outcome groups were higher in the 57 grids with no monitors than in the 15 grids with monitors. For each of the four health outcome groups, approximately 25% of observations were cases and about 75% were controls. The ratio of one case to three controls was also evident in grids with and without air monitors for ED asthma, IP asthma, IP MI, and IP HF (all p's>0.05). Only for ED asthma was the total (%) for Black patients (22696, 48%) higher than the totals (%) for White patients (21294, 45%) and Other patients (3060, 6%). For IP asthma, IP MI, and IP HF the totals (%) were highest for White patients, intermediate for Black patients, and lowest for Other patients. The Race by CMAQ grid condition analyses were significant for all four health outcomes (all p's≤0.05). ED asthma and IP asthma Black patients' totals (%) were higher in grids with air monitors than in grids

without air monitors, while this relationship was reversed for Other patients and White patients (all *p*'s≤0.05). As seen at the bottom of Table 4, IP MI and IP HF Black patients, Other patients, and White patients had higher totals (%) in grids without air monitors than in grids with air monitors (all *p*'s≤0.05).

CLR Analyses

CLR results showed significant differences between AOD-$PM_{2.5}$ and PMB fused surfaces, health outcome groups, lag grids, monitor conditions, and warm-cold season differences. For all CLR runs, ORs were significant at lag grids 0, 1, 01 and 04 (all *p*'s≤0.05). Effect modifiers were significant only for ED asthma in all grids (PMCQ population density, lag grid 0, protective OR, *p*≤0.05) and in grids with monitors (PMB, PMC, PMCK, PMCQ, PMCKQ fused surfaces for season, lag grids 2-4, 04, all *p*'s≤0.05). By using the mean (95% CI) it was possible to evaluate OR differences for the four health outcomes, four AOD-$PM_{2.5}$ and PMB fused surfaces at lag grids 0, 1, 01 and 04.

ED Asthma

Figure 1 shows ED asthma ORs (95% CIs) for the four AOD-$PM_{2.5}$ and PMB fused surfaces. There are separate panels in Figure 1, one for each of the four lag grid values

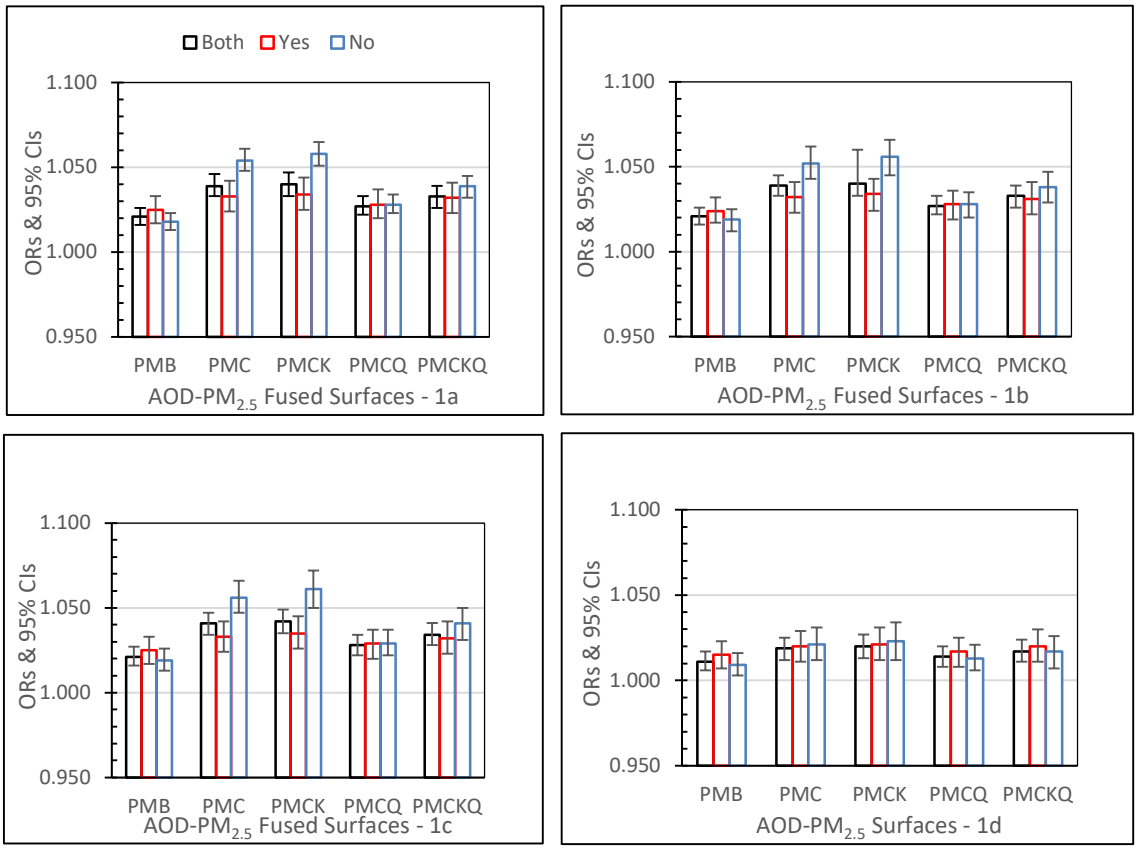

Figure 1: ED asthma ORs (95% CIs) for the four AOD-$PM_{2.5}$ and PMB fused surfaces, in all grids (Both) and in grids with (Yes) and without (No) air monitors, and in separate panels for lag grids 0 (1a), 1 (1b), 01 (1c), and 04 (1d).

of 0, 1, 01 and 04. In the Both grid condition, for lag grids 0, 1 and 01, ORs for each of the four AOD-$PM_{2.5}$ fused surfaces were significantly higher than the PMB ORs (all *p*'s≤0.05). In the Both grid condition, for lag grid 04, the PMC, PMCK and PMCKQ ORs were significantly higher than the PMB ORs (all *p*'s≤0.05). In lag grids 0, 1, and 01, the no monitor PMC and PMCK ORs were significantly higher than monitor PMC and PMCK ORs (all *p*'s≤0.05).

IP Asthma

Figure 2 shows IP asthma ORs (95% CIs) for the four AOD-$PM_{2.5}$ and PMB fused surfaces, and in separate panels for lag grids 0, 1, 01 and 04. In the Both grid condition, for lag grids 0, 1 and 01, the PMC, PMCK, and PMCKQ ORs were significantly higher than

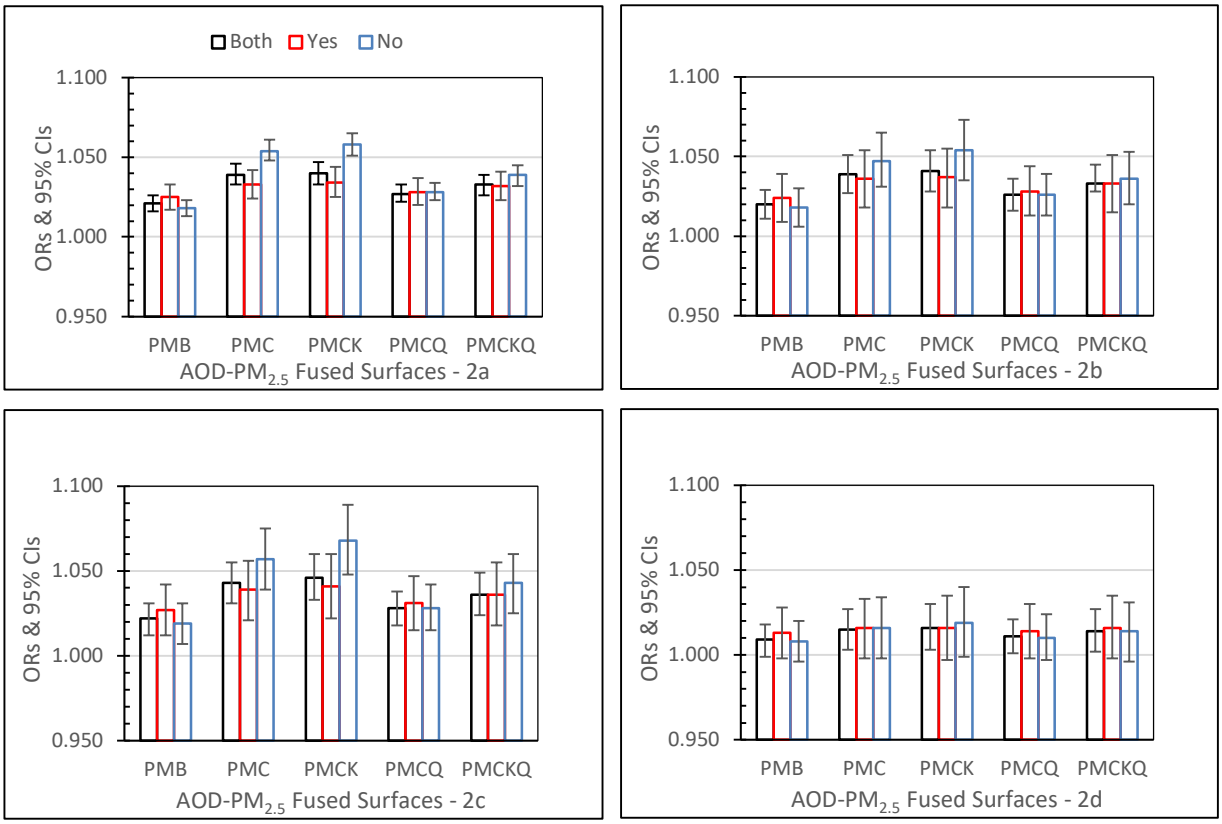

Figure 2: IP asthma ORs (95% CIs) for the four AOD-$PM_{2.5}$ and PMB fused surfaces, in all grids (Both), and in grids with (Yes) and without (No) air monitors, and in separate panels for lag grids 0 (2a), 1 (2b), 01 (2c) and 04 (2d).

the PMB ORs (all p's≤0.05). In lag grids 0 and 01, only the no monitor the PMCK ORs were significantly higher than the monitor PMCK ORs (both p's≤0.05).

IP MI

IP MI ORs for the four AOD-$PM_{2.5}$ and PMB fused surfaces, for lag grids 0, 1, 01 and 04, are displayed in Figure 3. In lag grids 0, 1 and 01, the PMC, PMCK, and PMCKQ ORs were significantly higher than PMB ORs (all p's≤0.05). Also in lag grids 0, 1 and 01, the no monitor PMC and PMCK ORs were significantly higher than the monitor PMC and PMCK ORs (all p's≤0.05).

Preprints (www.preprints.org) | NOT PEER-REVIEWED | Posted: 10 January 2022 doi:10.20944/preprints202201.0118.v1

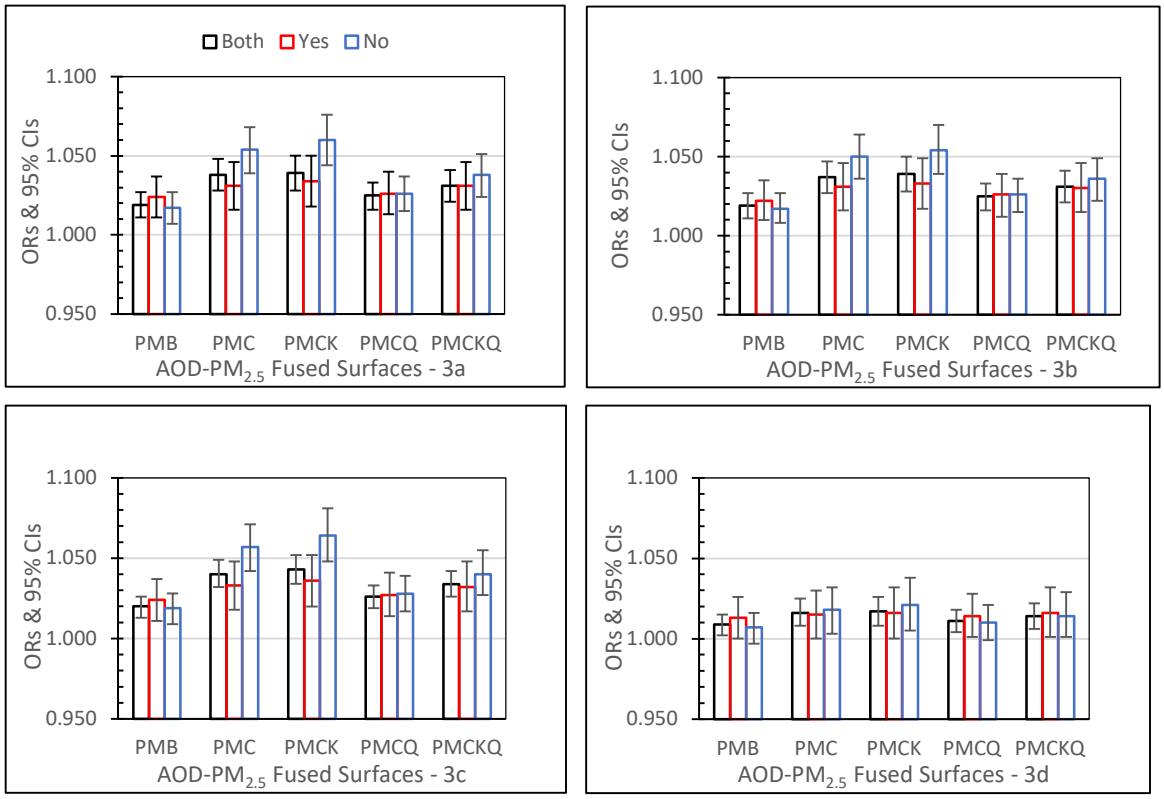

Figure 3: IP MI ORs (95% CIs) for the four AOD-$PM_{2.5}$ and PMB fused surfaces, in all grids (Both) and grids with (Yes) and without (No) air monitors, and in separate panels for lag grids 0 (3a), 1 (3b), 01 (3c) and 04 (3d).

IP HF

IP HF ORs for the five fused surfaces, three grid conditions and four lag grid values are displayed in Figure 4. In lag grids 0, 1 and 01, the PMC, PMCK, and PMCKQ ORs were significantly higher than PMB ORs (all p's≤0.05). For lag grid 04, only the PMCK OR was significantly higher than the PMB OR (p≤0.05). In lag grids 0, 1 and 01, the no monitor PMC and PMCK ORs were significantly higher than monitor PMC and PMCK ORs (all p's≤0.05).

Preprints (www.preprints.org) | NOT PEER-REVIEWED | Posted: 10 January 2022 doi:10.20944/preprints202201.0118.v1

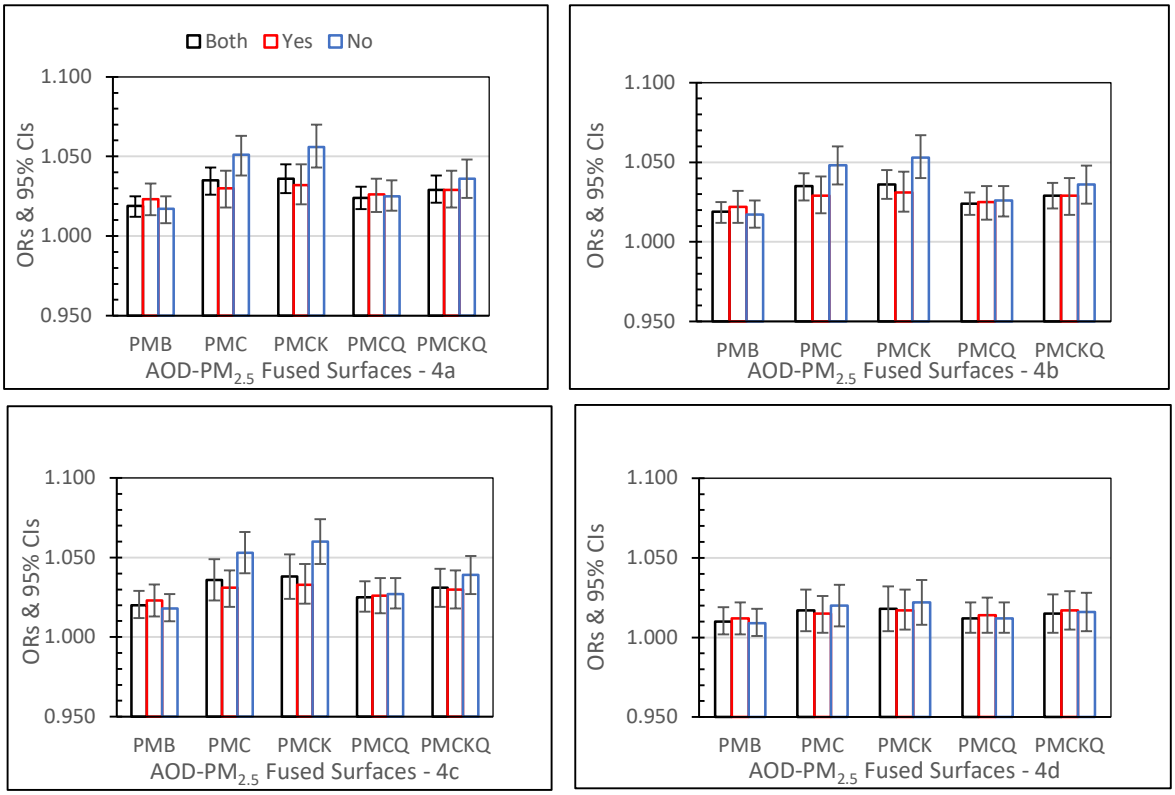

Figure 4: IP HF ORs (95% CIs) for the four AOD-PM2.5 and PMB fused surfaces, in all grids (Both), and in grids with (Yes) and without (No) air monitors, and in separate panels for lag grids 0 (4a), 1 (4b), 01 (4c) and 04 (4d).

Monitor Versus No Monitor OR Percent

The no monitor – monitor OR percent (ΔOR%) values for the four AOD-PM2.5 and PMB fused surfaces and four lag grids 0, 1, 01 and 04, are displayed, in four separate panels, one for each of the four health outcomes, in Figure 5. For the four health outcomes, ΔOR% values were larger for PMC and PMCK than the other three fused surfaces. These differences occurred for each one of the four lag grid values. The ΔOR% values at lag 04 was smaller than the ΔOR% values at lag grids 0, 1 and 01. For the four health outcomes, PMB ΔOR% values were negative at lag grids 0, 1, 01 and 04. Results were mixed for PMCQ and PMCKQ. IP asthma PMCQ had negative ΔOR% values as did IP asthma PMB. PMCKQ ΔOR% at lag grids 0, 1 and 01 were positive, resembling PMC and PMCK. One difference, however, was the PMCKQ ΔOR% values were lower than the PMC and PMCK ΔOR% values at lag grid 04. PMCQ ΔOR% values were negative for ED asthma and IP asthma, resembling PMB ED asthma and IP asthma ΔOR% values.

Preprints (www.preprints.org) | NOT PEER-REVIEWED | Posted: 10 January 2022 doi:10.20944/preprints202201.0118.v1

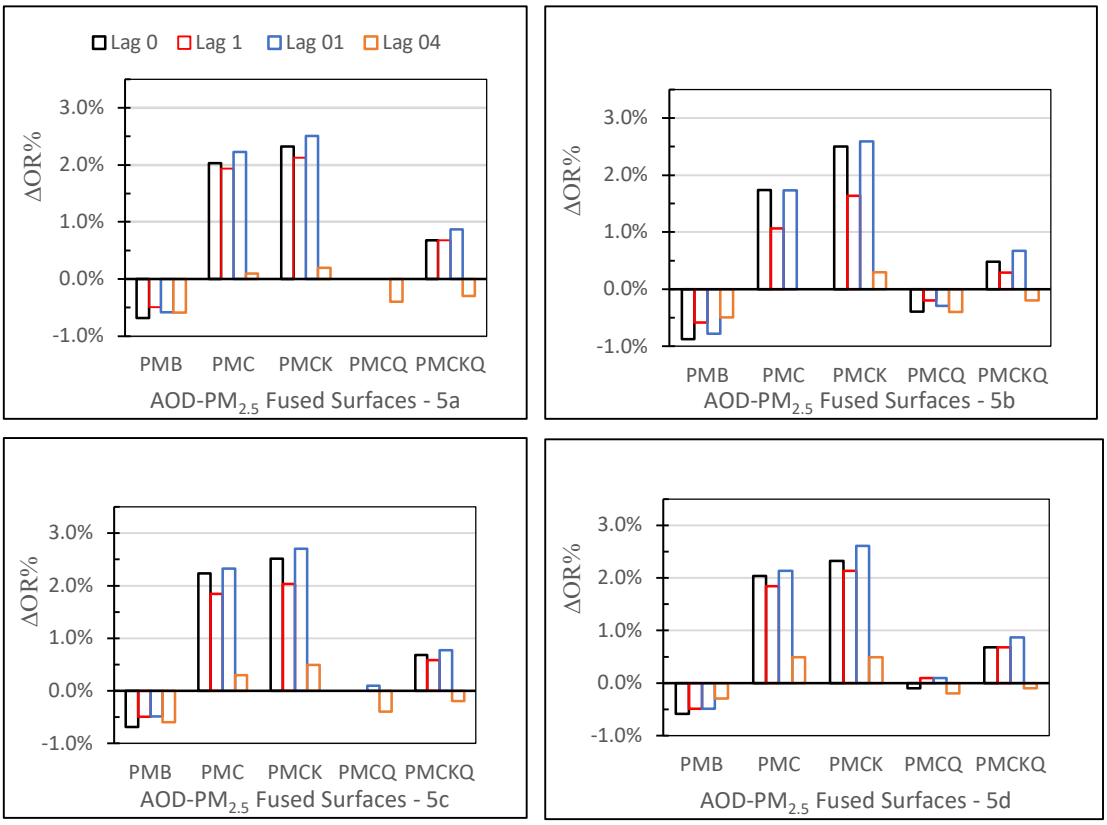

Figure 5: No monitor – Monitor percent (ΔOR%) results for the four AOD-PM2.5 and PMB fused surfaces for lag grids 0, 1, 01 and 04, and in separate panels for ED asthma (5a), IP asthma (5b), IP MI (5c), and IP HF (5d).

Size of Homogeneous Spatial Area

The largest size of the homogeneous spatial area was identified by the presence of a significantly higher AOD-PM2.5 fused surface OR than the PMB OR for each chronic disease group (ED asthma, IP Asthma, IP MI, and IP HF) at lag grids 0, 1, 01 and 04. Table 5 summarizes the homogeneous spatial area findings. For both monitor grid conditions combined (Both, top of Table 5) analyses of ED asthma and IP HF with the PMCK fused surface produced ORs that were significantly higher than the PMB ORs at lag grid values of 0, 1, 01 and 04 (all p's≤0.05). ORs for ED asthma with the PMC and PMCKQ fused surfaces were significantly higher than the PMB ORs at lag grids 0, 1, 01 and 04 (all p's≤0.05). Based on these significant outcomes at lag grid 04 for these three AOD-PM2.5 fused surfaces, it was concluded that the largest homogeneous spatial area for PMC, PMCK and PMCKQ fused surfaces was (1 grid 12 km wide x 5 grids) 60 km wide. In grids with air monitors, only the ED asthma PMCK ORs were significantly higher than the PMB ORs for lag grids 0, 1 and 01 (all p's≤0.05). The width of the largest homogeneous spatial area for PMCK was 2 grids wide, or 24 km. In grids without air monitors the analyses of ED asthma, IP MI, and IP HF with the PMC and PMCK fused surfaces produced ORs that were significantly higher than PMB ORs at lag grids 0, 1, 01 and 04 (all p's ≤0.05). The analyses of ED asthma with PMCKQ resulted in ORs that were significantly higher than the PMB ORs at lag grids 0, 1, 01 and 04 (all p's≤0.05). The maximum size of the homogeneous spatial area for PMC, PMCK and PMCKQ was 5 grids wide.

Table 5: Lag Grid Analyses Identified the Size of Homogeneous Spatial Areas, in Multiples of one 12 km-wide CMAQ Grid, Where AOD-$PM_{2.5}$ Fused Surface Concentration Level is Greater than PMB Concentration Level (Top), and AOD-$PM_{2.5}$ and PMB Fused Surface Concentration Level Differences Between Grids With Air Monitors and Grids Without Air Monitors (Bottom).

GRID MONITORS[1]	CHRONIC DISEASE GROUPS			
	ED Asthma	IP Asthma	IP MI	IP HF
Both				
PMC	4 (0, 1, 01, 04)	3 (0, 1, 01)	3 (0, 1, 01)	3 (0, 1, 01)
PMCK	4 (0, 1, 01, 04)	3 (0, 1, 01)	3 (0, 1, 01)	4 (0, 1, 01, 04)
PMCQ	0	0	0	0
PMCKQ	4 (0, 1, 01, 04)	3 (0, 1, 01)	3, (0, 1, 01)	3 0, 1, 01)
Yes				
PMC	0	0	0	0
PMCK	2 (0, 1, 01)	0	0	0
PMCQ	0	0	0	0
PMCKQ	0	0	0	0
No				
PMC	4 (0, 1, 01, 04)	3 (0, 1, 01)	4 (0, 1, 01, 04)	4 (0, 1, 01, 04)
PMCK	4 (0, 1, 01, 04)	3 (0, 1, 01)	4 (0, 1, 01, 04)	4 (0, 1,01, 04)
PMCQ	3 (0, 1, 01)	0	0	0
PMCKQ	4 (0, 1, 01, 04)	3 (0, 1, 01)	3 (0, 1, 01)	3 (0, 1, 01)
Monitor-No Monitor[2]				
PMB	=	=	=	=
PMC	< (0, 1, 01)	< (1, 01)	< (0, 1, 01)	< (0,1, 01)
PMCK	< (0, 1, 01)	< (0, 01)	< (0, 1, 01)	< (0, 1, 01)
PMCQ	=	=	=	=
PMCKQ	=	=	=	=

[1]Each AOD-$PM_{2.5}$ fused surface mean is compared with PMB fused surface mean (95% CI). Only significant differences are shown, $p \leq 0.05$. [2]AOD-$PM_{2.5}$ and PMB fused surface means in grids without air monitors are compared to means (95% CI) in grids with air monitors. Significant outcome at $p \leq 0.05$ is displayed with symbol of "<". Not significant outcome for $p > 0.05$ is shown with symbol of "=".

Monitor-No Monitor Differences

The purpose of these analyses was to determine if the AOD-$PM_{2.5}$ and PMB fused surfaces had concentration levels that differed between grids with and without air monitors. Results are presented at the bottom of Table 5. The ORs for ED asthma, IP asthma, IP MI, and IP HF with PMC and PMCK fused surfaces were significantly higher in rural grids without air monitors than in urban grids with air monitors (all p's≤ 0.05).

Warm-Cold Season

There were warm-cold season differences for the four the AOD-$PM_{2.5}$ fused surfaces and the four health outcomes (Online Resource includes electronic supplementary material consisting of Figures S1 [ED asthma: a-d, lag grids 0, 1, 01, 04, respectively] though S4 [IP HF: a-d, lag grids 0, 1, 01, 04, respectively] for ED asthma (referenced), IP asthma, IP MI, and IP HF (referenced); EMS_1,pdf file). These outcomes were expressed as larger ORs during the warm season and smaller ORs during the cold season. Specifics for each health outcome will be presented below.

ED asthma (Figure S1), IP asthma (Figure S2), and IP MI (Figure S3) PMB, PMC, PMCK, PMCQ, and PMCKQ warm season ORs were significantly higher than cold season ORs for lag grids 0, 1 and 01 (all p's≤ 0.05). ED asthma, IP asthma, and IP MI PMCK warm season ORs were significantly higher than cold season ORs for lag grid 04 (all

 doi:10.20944/preprints202201.0118.v1

p's≤0.05). IP HF PMB, PMC, PMCK, PMCQ and PMCKQ warm season ORs were significantly higher than cold season ORs for lag grids 0, 1, 01 and 04 (all *p's*≤0.05).

Table 6 shows the three-year mean (95% CI) $PM_{2.5}$ concentration levels for the four AOD-$PM_{2.5}$ and PMB fused surfaces and three-year mean ambient temperature values in F° by season (Both, Warm, Cold). The Both condition shows the significant correlations

Table 6: Three-Year Means (95% CIs) for AOD-$PM_{2.5}$ and PMB Fused Surfaces and Ambient Temperature, and Correlations Between Fine PM and Temperature, by Monitor Status (Both, No and Yes) in Rows and Season (Both, Warm, Cold) in Columns, Baltimore Study Area Lag Grid Analyses.

Variables[a-b]	Season		
	Both	Warm	Cold
Monitors – Both			
PMB	14.19 (14.13-14.26) [4.6]‡	14.89 (14.81-14.96)†	13.50 (13.41-13.60)
PMC	13.66 (13.60-13.72) [40.7]‡	15.29 (15.21-15.38)†	12.03 (11.97-12.08)
PMCK	14.38 (14.31-14.44) [59.3]‡	16.65 (16.57-16.74)†	12.10 (12.06-12.14)
PMCQ	13.79 (13.73-13.85) [10.4]‡	14.69 (14.61-14.76)†	12.90 (12.82-12.99)
PMCKQ	13.91 (13.85-13.97) [37.3]‡	15.52 (15.44-15.59)†	12.31 (12.25-12.36)
Temperature (F°)	55.86 (55.55-56.18)	68.97 (68.77-69.16)†	42.76 (42.55-42.96)
Monitors – No			
PMB	14.12 (14.05-14.19) [3.6]‡	14.80 (14.71-14.88)†	13.45 (13.34-13.55)
PMC	13.62 (13.55-13.68) [41.3]‡	15.26 (15.17-15.35)†	11.97 (11.92-12.03)
PMCK	14.39 (14.32-14.47) [61.2]‡	16.72 (16.63-16.82)†	12.06 (12.03-12.10)
PMCQ	13.71 (13.64-13.77) [9.3]‡	14.59 (14.51-15.57)†	12.83 (12.74-12.92)
PMCKQ	13.85 (13.79-13.92) [37.8]‡	15.49 (15.41-15.57)†	12.22 (12.16-12.28)
Temperature (F°)	55.60 (55.26-55.94)	68.68 (68.46-68.89)†	42.53 (42.31-42.75)
Monitors – Yes			
PMB	14.60 (14.44-14.76) [11.2]‡	15.38 (15.17-15.60)†	13.81 (13.59-14.03)
PMC	13.90 (13.73-14.06) [37.1]‡	15.46 (15.23-15.69)†	12.33 (12.17-12.49)
PMCK	14.27 (14.10-14.44) [50.2]‡	16.25 (16.02-16.47)†	12.30 (12.16-12.43)
PMCQ	14.28 (14.12-14.43) [16.5]‡	15.24 (15.03-15.46)†	13.31 (13.11-13.51)
PMCKQ	14.24 (14.09-14.40) [34.0]‡	15.69 (15.48-15.90)†	12.79 (12.63-12.96)
Temperature (F°)	57.32 (56.50-58.13)	70.61 (70.11-71.11)†	44.02 (43.54-44.51)

[a]Significance for warm vs. cold season $PM_{2.5}$ concentration level values and correlations between fine PM and temperature for the five fused surfaces: †p≤0.05, ‡p≤0.01. [b]The $r^{2\%}$ for each correlation is in brackets.

between each fused surface $PM_{2.5}$ concentration level and ambient temperature (all *p's*≤0.05). The measure of association shown is $r^{2\%}$, the square of the correlation (r) expressed as a percent. The $r^{2\%}$ value quantifies the percentage of the variance that is shared by each fused surface $PM_{2.5}$ concentration level and ambient temperature. The $r^{2\%}$ measures are largest for PMCK, smallest for PMB and PMCQ, and intermediate for PMC and PMCKQ, in all three monitor grid conditions (Both, No, Yes). PMB $r^{2\%}$ was higher in grids with monitors (11.2%) and lower in grids without monitors (3.6%). PMCQ's $r^{2\%}$ was also higher in grids with monitors (16.5%) than in grids without monitors (9.3%). Differences in the $r^{2\%}$ measure between grids without and with air monitors were positive for PMC (41.3%-37.1% = 4.2%), PMCK (61.2%-50.2% = 11%), and PMCKQ (37.8%-34.0% = 3.8%), and negative for PMB (3.6%-11.2% = -7.6%) and PMCQ (9.3%-16.5% =-7.2%) . Concentration levels for the five $PM_{2.5}$ fused surfaces were significantly higher during the warm season than during the cold season, under all three grid conditions (all *p's*≤0.05). As expected, ambient temperature during the warm season was significantly higher than during the cold season for the three grid conditions (all *p's*≤0.05).

Preprints (www.preprints.org) | NOT PEER-REVIEWED | Posted: 10 January 2022 doi:10.20944/preprints202201.0118.v1

Warm Versus Cold Season OR Percent

Figure 6 displays the warm – cold season ΔOR% values. The ΔOR% measures were positive for each of the four AOD-$PM_{2.5}$ and PMB fused surfaces, for ED asthma (panel a), IP asthma (b), IP MI (c), and IP HF (d) in lag grids 0, 1, 01, and 04. All four panels in Figure 6 demonstrate that PMC and PMCK had consistently higher ΔOR% values than the other two AOD-$PM_{2.5}$ (PMCQ, PMCKQ) and the baseline PMB fused surfaces at lag grids of 0, 1, and 01. ED asthma ΔOR% values were smaller than the ΔOR% values for IP asthma, IP MI, and IP HF. Also, for all four health outcomes and the four AOD-$PM_{2.5}$ and PMB fused surfaces, ΔOR% values were smaller at lag grid 04 than at the other three lag grid values of 0, 1, and 01.

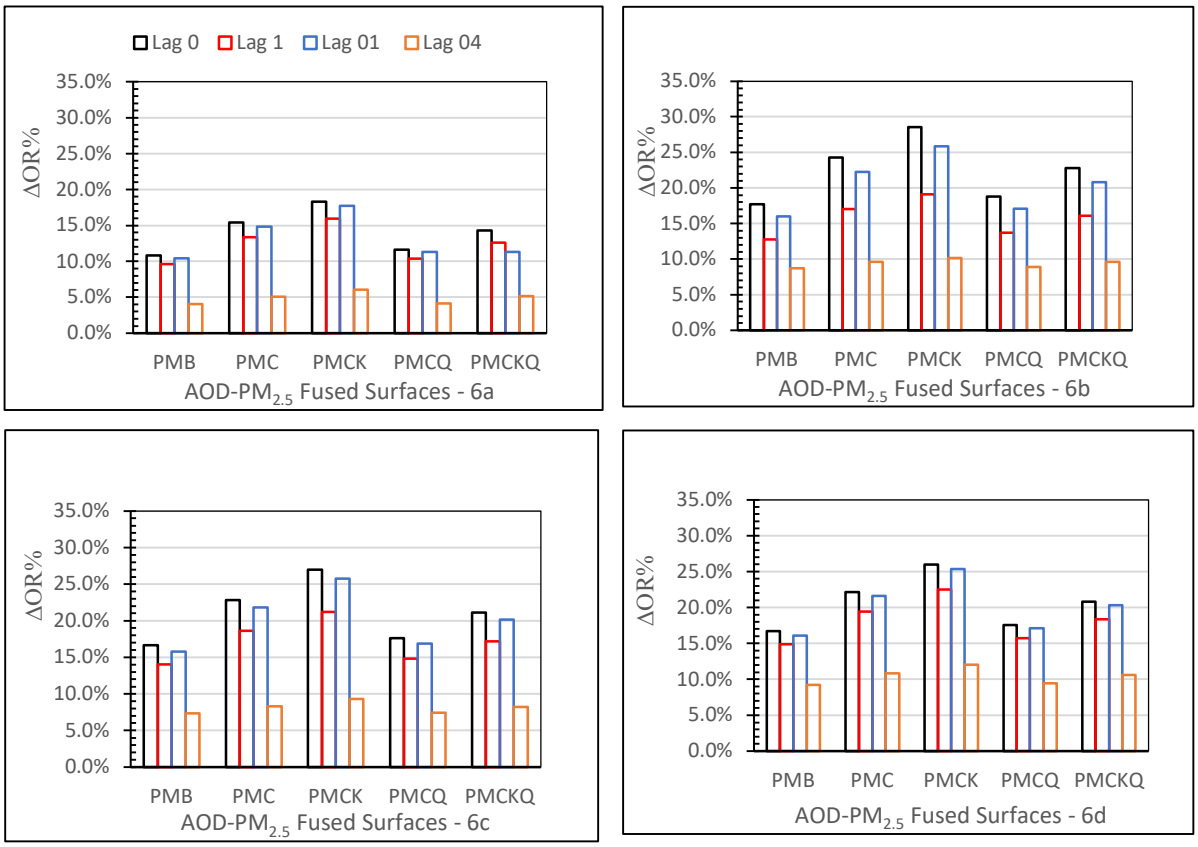

Figure 6: Warm season – cold season ΔOR% values for the four AOD-$PM_{2.5}$ and PMB fused surfaces at lag grids 0, 1, 01 and 04 for ED asthma (6a), IP asthma (6b), IP MI (6c), and IP HF (6d), in different panels.

4. Discussion

This data analysis study implemented, for the first time, a spatial lag grid case-crossover design to identify homogeneous spatial areas in rural grids without air monitors that displayed a similar association between elevated AOD-$PM_{2.5}$ and PMB concentration levels and increases in respiratory-cardiovascular ED visits and IP hospitalizations as has been found in urban grids with air monitors. Analyses of ED asthma, IP MI, and HP HF with PMC and PCMCK attained a maximum homogeneous spatial area (12 km * 12 km * 5 grids [0-4]) of 720 km^2. The largest homogeneous spatial area identified by the analysis of ED asthma with PMCKQ was also 720 km^2.

The homogeneous spatial area analysis results for the Baltimore study area, urban grids with air monitors and rural grids without air monitors combined, were the same as those obtained for the no monitor grid analyses. For the urban area air monitor grid condition, the comparisons between each of the four AOD-$PM_{2.5}$ fused surfaces and PMB were not significant, except for the analysis of ED asthma with PMCK at lag grids 0, 1 and 01.

These results indicate that the benefit of utilizing AOD-$PM_{2.5}$ is only detected when the analyses are completed in grids without air monitors. Other analyses demonstrated what combinations of the four AOD-$PM_{2.5}$ and PMB fused surfaces with the four respiratory-cardiovascular hospital events resulted in larger ORs in rural grids without air monitors and smaller ORs in urban grids with air monitors. PMC and PMCK ED asthma, IP asthma, IP MI, and IP HF ORs in grids without air monitors were significantly higher than ORs in grids with air monitors at lag grids 0, 1 and 01. There were differences in the pattern of significant ORs obtained with the spatial lag grid case-crossover design used in this study and the temporal lag day case-crossover design reported by Braggio and associates in 2020 [3]: For the temporal case-crossover analyses only lag days 0, 1 and 01 were significant. The implementation of the spatial case-crossover analyses in this study obtained significant lag grids of 0, 1, 01 and 04.

Categorical analyses of Baltimore study area demographics identified, for the first time, a subset of homogeneous spatial grids in rural areas without ambient air monitors that resembled urban grids with ambient air monitors in poverty percent and population density: In rural areas there were 8 grids with poverty percent values in the Above category, and 7 grids in urban areas with poverty percent values in the Above category. There were 19 rural grids with population density in the Above category and 11 urban grids in the above category. In addition, there were higher totals and percentages of IP MI (12016, 62.6%) and IP HF (15684, 57.0%) in rural areas than in urban areas (7185, 37.4% and 11834, 43.0%, respectively). But the totals and the percentages of Black ED asthma patients (11844, 25.2%) and IP asthma patients (2358, 17.5%) were higher in urban areas than in rural areas (10852, 23.1% and 2152, 16.0%, respectively). These results support the conclusion that within the Baltimore study area there is a subset of rural grids without air monitors that resembles the set of 15 urban grids with air monitors in demographic risk factors and in the association between elevated AOD-$PM_{2.5}$ concentration levels and increases in respiratory-cardiovascular ED visits and IP hospitalizations.

In an epidemiologic study Hirshon and associates [40] evaluated $PM_{2.5}$ concentration and zinc level readings from the Baltimore $PM_{2.5}$ Supersite and children's asthma ED visits and IP hospitalizations. These authors reported that $PM_{2.5}$ zinc concentrations resulted in increases in asthma hospital events. The publication did not identify the zinc source, however. One explanation could be that the ambient $PM_{2.5}$ zinc levels recorded at the Baltimore $PM_{2.5}$ Supersite [130] may have come, in part, from a nearby TRI site [131].

The Baltimore $PM_{2.5}$ Supersite location can be remapped onto one of the 99 CMAQ grids utilized in the Baltimore study area [3]. As a result of this remapping, we discovered that the location of the Baltimore $PM_{2.5}$ Supersite is in CMAQ grid R_6, C_6. This same Baltimore study area grid also had three FRM $PM_{2.5}$ air monitors and one EPA-identified TRI facility that emitted ambient zinc fumes and dust. An adjacent Baltimore study area, grid R_6, C_7, had one TRI facility that released zinc fumes and dust in the air.

As a follow-up to the Hirshon and associates [40] study, we also looked at the number of TRI facilities that released zinc fumes or dust in the Baltimore study area between 2004-2006. There were five different businesses operating during this three-year timeframe. One company had facilities in two distinct locations, contributing a total of 11 zinc point sources: 7 zinc fumes or dust point sources in grids with air monitors (urban grids) and four in grids without air monitors (rural grids). This analysis suggests that the ambient $PM_{2.5}$ zinc measured at the Baltimore $PM_{2.5}$ Supersite in 2002 could have originated, at least in part, from a nearby TRI facility that emitted zinc fumes and dust. Although the FRM $PM_{2.5}$ air monitors data we utilized did not include $PM_{2.5}$ zinc, it is possible that ambient zinc from TRI zinc emitting facilities in selected at-risk grids (with or without air monitors) in the Baltimore study area could have contributed to children's asthma ED visits and IP hospitalizations.

Although this study did not evaluate the environmental hazard associated with living close to brownfields [132, 133] or EPA-designated Toxic Release Inventory (TRI) facilities [131], several published studies have described the environmental contamination

from manufacturing efforts in Maryland that have included the EPA TRI facilities in the State [134-137] and brownfields in South Baltimore [132, 133]. Perlin, Sexton, and Wong [135] found that there were 122 TRI sites in Maryland. About half of the TRI facilities were in Baltimore City, Howard, Anne Arundel, and Baltimore Counties. Maryland residents near a TRI site were medically underserved [137]. South Baltimore brownfields have higher respiratory and heart disease mortality rates among White working-class residents than the rest of the City and State [132]. Litt, Tran, and Burke [133] described a variety of environmental hazards in Southeast Baltimore that included heavy metals, solvents, and insecticides. Living in these environmentally-compromised areas for long durations could increase residents' adverse responsiveness to lower ambient $PM_{2.5}$ concentration levels and their enhanced contribution to respiratory-cardiovascular ED visits or IP hospitalizations [5, 24, 132, 133].

The suggestion introduced here is that the accuracy of AOD-$PM_{2.5}$ concentration levels in estimating actual ambient $PM_{2.5}$ concentration levels determined by on-the-ground fine PM ambient air monitors is partly contingent on spatial scale [44, 68, 138-140]. Remote sensing studies that have used AOD to estimate ambient $PM_{2.5}$ concentration levels have concluded that smaller grids provide greater accuracy than larger grids. We utilized the NASA 10 km^2 grid when we accessed the AOD unitless readings for the Baltimore and New York City study areas. Since our objective has been to evaluate how accurately the four experimental AOD-$PM_{2.5}$ concentration level fused surfaces, in comparison to baseline PMB, estimated ambient $PM_{2.5}$ concentration levels and their contribution to the occurrence of respiratory-cardiovascular chronic disease ED visits and IP hospitalization in all grids and grids with and without ambient air monitors, the NASA 10 km^2 grid was mapped to the EPA CMAQ 12 km^2 grid before the Baltimore and New York City epidemiologic studies were undertaken [3, 32, 84]. In the Braggio and associates' publications [3, 84] and the results of this study, we have controlled for scale effects on the accuracy of AOD-$PM_{2.5}$ fused surfaces to represent actual ambient $PM_{2.5}$ concentration levels by utilizing the EPA CMAQ 12 km^2 grid as the smallest spatial area of analysis. The larger sites, those that defined grid multiples with air monitors, grid groups without air monitors, and both air monitor grid conditions combined, are not less accurate than the individual 12 km^2 grid since the larger areas represent the inclusion of multiple homogeneous 12 km^2 grids into larger spatial grid areas. Likewise, the accuracy of the identified homogeneous spatial areas, in rural grids without air monitors and in urban grids with air monitors, is equivalent to the accuracy which characterizes each CMAQ grid.

Previously published studies have also found higher $PM_{2.5}$ concentration levels and worse health outcomes during the warm season than during the cold season [3, 10, 18, 31], while other reports have reported larger cold season effects and smaller warm season effects [7, 13, 28, 32, 41, 97, 98]. Cheng and colleagues [8] found significant increases in asthma hospital admissions on warm (>23° C) and cool (<23° C) days in Taipei, Taiwan. Our analyses found significant positive associations between AOD-$PM_{2.5}$ concentration levels and ambient temperature, suggesting that higher temperatures during the warm season, relative to the cold season temperatures, contributed to the increased OR of respiratory-cardiovascular ED visits and IP hospitalizations. In grids with and without air monitors, the $r^{2\%}$ values were higher for PMCK than the other three AOD-$PM_{2.5}$ and PMB fused surfaces. This measure of association between PMCK and ambient temperature explained 59% of the shared variance in all grids, 61% in grids without air monitors, and 50% in grids with air monitors. Results for PMC-ambient temperature shared variance were 41% in the Baltimore study area, 41% in grids without air monitors, and 37% in grids with air monitors. Percentages of fused surface-ambient temperature shared variance measured by $r^{2\%}$ were smaller for PMB: 4.6% in the Both condition, 3.6% in grids without air monitors, and 11.2% in grids with air monitors. The association between AOD-$PM_{2.5}$ concentration level and ambient temperature could be a proxy for another factor that could contribute to increases in ambient fine PM concentration levels: Possible fine PM sources could include transportation and manufacturing air pollution particles [141, 142].

Therefore, these warm-cold season results also support using the PMC or the PMCK fused surface as a candidate to replace PMB, the currently available baseline, as a reliable and accurate estimate of ambient $PM_{2.5}$ concentration level.

These spatial lag grid results provide additional support for the use of PMC and PMCK fused surfaces in epidemiologic investigations of the association between ambient fine PM and respiratory-cardiovascular hospital events. Both PMC and PMCK consistently identified OR differences between air monitor and no air monitor grids relative to the mixed results for the other two fused surfaces that included $PM_{2.5}$ CMAQ model estimates, PMCQ and PMCKQ. PMC and PMCK showed larger changes between warm and cold season ORs. Published studies have contributed to the continued improvement in the use of remote sensing methodology by showing how AOD can be utilized to more accurately estimate ambient $PM_{2.5}$ concentration levels in areas with and without air monitors [3, 6, 9, 13-16, 20, 22, 30, 32, 48, 51, 52, 54, 57-74, 77, 80-82, 84, 89, 92, 143]. Based on the results of this study, spatial attributes favor the use of PMCK over PMC as the replacement for PMB.

There are strengths in the analytical methods utilized in this spatial lag grid case-crossover study. To our knowledge, this is the first time the case-crossover design has been modified to evaluate lag grids. The selection of controls that preceded or followed the cases makes the lag grid case-crossover design spatially bidirectional [105]. The use of the lag grid case-crossover design to quantify spatial heterogeneity provides an assessment tool to identify homogeneous spatial areas. Study results demonstrate, also for the first time, the presence of grids without air monitors (rural grids) that resembled grids with air monitors (urban grids) in exposing rural residents to increased fine PM levels and seeking medical care for a respiratory-cardiovascular chronic disease hospital events. A final contribution of this study was the identification of benefits derived by utilizing AOD-$PM_{2.5}$ concentration level fused surfaces, especially PMCK, as estimates of ambient fine PM levels in urban and rural areas.

There are unresolved methodological issues that limit the generalizability of study results. The 99 CMAQ grids that defined the Baltimore study area included 15 urban grids with air monitors and 84 rural grids without air monitors. All 15 urban grids with monitors had associated respiratory-cardiovascular hospital event data. Only 57 of the 84 rural grids without air monitors had respiratory-cardiovascular hospital event data. Grids without air monitors that lacked health data could have been those grids over the Chesapeake Bay. The Chesapeake Bay CMAQ grids, located in the south-east corner of the Baltimore study area, included more water than land mass. Residents live on part of Maryland's irregular coastline and islands. Underestimates for total patients with respiratory-cardiovascular ED visits and IP hospitalizations could have occurred because Maryland residents can and do obtain medical treatment out of state, e.g., Washington, DC, Virginia, Pennsylvania. To be consistent with the way the linear boundaries for the New York City study area and the Baltimore study area were established for the purpose of developing the AOD-$PM_{2.5}$ and PMB fused surfaces, it was necessary to include all 99 CMAQ grids in the Baltimore study area. Another study limitation was the inability to identify which grids were included in the homogeneous spatial areas. Based on the way this study implemented the spatial lag grid case-crossover design, only the size of the homogeneous spatial area could be determined as CMAQ grid multiples, with each one 12 km wide. There was no independent confirmation of actual ambient $PM_{2.5}$ concentration levels in rural grids without air monitors. There was also (relative) spatial heterogeneity in the 15 urban grids with air monitors because there were only 17 ambient air monitors for an area of (12 km * 12 km * 15 grids) 2160 km^2. If the 17 fine PM ambient air monitors were equally distributed among the 15 CMAQ grids, each monitor would occupy 127.1 km^2. Monitor accuracy for the fine PM measurements is highest at the monitor's location. Fine PM measurement accuracy decreases as the distance from the monitor increases. It is not clear to what extent health care access impacted the results. Available evidence indicated that this may not have been a bias since there were more patients

with the four respiratory-cardiovascular chronic diseases in rural grids without air monitors than in urban grids with air monitors.

Future research efforts should involve the identification of criteria that will lead to the replacement of the currently used PMB baseline fused surface with another improved AOD-$PM_{2.5}$ fused surface. Relevant attributes that could be helpful in the selection of an updated AOD-$PM_{2.5}$ baseline can include grid resolution below 10 km^2, absence of missing AOD unitless readings, and improved accuracy of $PM_{2.5}$ concentration level estimates in areas without ambient air monitors [3, 84]. In addition, to increase the reliability and validity of $PM_{2.5}$ readings in grids without air monitors [84], it will be necessary to have available, independent on-the-ground ambient $PM_{2.5}$ readings in grids without ambient air monitors. This more ambitious goal could be reached by using portable and accurate $PM_{2.5}$ monitors to supplement fine PM readings available from the EPA AQS network [50]. The overall goal of these proposed improvements will be to protect the respiratory-cardiovascular health of residents in rural areas, as has been accomplished thus far for residents in urban areas.

5. Conclusions

The spatial lag grid case-crossover results provided support for the use of this analytical method to identify homogeneous spatial areas that demonstrated the same relationship between elevated AOD-$PM_{2.5}$ concentration levels and increased respiratory-cardiovascular hospital events in the entire Baltimore study area and in rural grids without air monitors. With the PMC and PMCK fused surfaces, the largest homogeneous spatial areas, showing the same relationship between elevated AOD-$PM_{2.5}$ and ED asthma and IP HF, were 720 km^2 for the Baltimore study area (Both) and in rural grids without air monitors. These results suggest that some rural grids without air monitors were not necessarily different from urban grids with air monitors in the contribution of increased ambient fine PM to the occurrence of respiratory-cardiovascular hospital events. While limitations in the spatial case-crossover analyses could not identify specific grids included in the homogeneous spatial areas, other results from categorical data analyses confirmed that there was a subset of rural grids without air monitors that demonstrated higher poverty percent, increased population density and elevated AOD-$PM_{2.5}$ concentration levels as has been found for urban grids with air monitors. Warm-cold season analyses confirmed that elevated AOD-$PM_{2.5}$ concentration levels during the warm season contributed to increases in respiratory-cardiovascular ED visits and IP hospitalizations. New information confirmed the association between elevated AOD-$PM_{2.5}$ concentration levels and ambient temperature. Higher temperatures could be proxies for other sources of fine PM that are more prevalent during the warm season than during the cold season. PMC and PMCK fused surfaces consistently demonstrated larger differences between warm and cold seasons than the other two AOD-$PM_{2.5}$ fused surfaces that included CMAQ $PM_{2.5}$ estimates (PMCQ and PMCKQ) or the currently used baseline, PMB. Future research efforts should reevaluate the contribution of increased ambient fine PM levels and area-specific demographic and environmental hazards to increased susceptibility of developing respiratory-chronic diseases especially in Maryland's rural areas, and rural areas in other locations.

Supplementary Materials: The following are available online at www.mdpi.com/xxx/s1, Four figures display warm-cold season odds ratios (ORs) at spatial lags 0, 1, 01 and 04, for each of the four AOD-$PM_{2.5}$ and PMB concentration level fused surfaces, four respiratory-cardiovascular emergency department and inpatient hospitalizations in all CMAQ 12 km^2 grids, and in grids with and without air monitors: Figure S1, ED asthma ORs and 95% CIs for the four AOD-$PM_{2.5}$ and PMB fused surfaces during the warm and cold seasons at lag grids 0 (S1a), 1 (S1b), 01 (S1c) and 04 (S1d); Figure S2, IP asthma ORs and 95% CIs for the four AOD-$PM_{2.5}$ and PMB fused surfaces during the warm and cold

seasons at lag grids 0 (S2a), 1 (S2b), 01 (S2c) and 04 (S2d); Figure S3, IP MI ORs and 95% CIs for the four AOD-$PM_{2.5}$ and PMB fused surfaces during the warm and cold seasons at lag grids 0 (S3a), 1 (S3b), 01 (S3c) and 04 (S3d); Figure S4, IP HF ORs and 95% CIs for the four AOD-$PM_{2.5}$ and PMB fused surfaces during the warm and cold seasons at lag grids 0 (S4a), 1 (S4b), 01 (S4c) and 04 (S4d).

Author Contributions: Conceptualization: JTB, AH, SW, EH; Methodology: JTB, AH, SW, EH; Software: EH; Validation, JTB, EH, SW, AH; Formal Analysis: JTB, AH, SW; Investigation: JTB; Resources: AH, SW, EH; Data Curation: JTB, EH; Writing—Original Draft Preparation: JTB; Writing—Review & Editing: JTB, EH, AH, SW; Visualization: JTB, AH; Supervision: AH, SW, EH, JTB; Project Administration: AH, SW, EH; Funding Acquisition: AH, SW, JTB. All authors have read and agreed to the published version of the manuscript.

Funding: Research supported by a National Aeronautics and Space Administration Grant (NNH11CD19C) for Earth Science Applications Feasibility Studies: Public Health awarded to Battelle Memorial Institute, Columbus, Ohio. The funding Agency was not involved in the study's design, analysis of the data, or the manuscript's writing.

Institutional Review Board Statement: The Maryland Department of Health Institutional Review Board and the Maryland Health Services Cost Review Commission approved the study's protocol to utilize the State's electronic hospital patient records, ED visits and IP hospitalizations, to complete the analyses described in this paper.

Informed Consent Statement: Not applicable.

Data Availability Statement: The Maryland Health Services Cost Review Commission provided one year's access to confidential hospital data, after payment of the data usage fee. It is not possible to share the electronic patient records since the electronic patient records contain information that could be used to identify the names and addresses of patients in the electronic ED and IP files.

Acknowledgments: Judy Qualters of the U.S. Centers for Disease Control and Prevention (CDC) endorsed and supported this data linkage and analysis project. Fred Dimmick, U.S. Environmental Protection Agency (EPA), facilitated the initial 'proof-of-concept' project for this inter-agency collaboration on this data linkage and analysis project, as well as two prior data linkage studies. Eric S. Hall, EPA, continued the formal inter-agency partnership between CDC and EPA on this data linkage and analysis project and was the co-developer of the HBM used in the New York City and Baltimore data analysis studies. Michelle Morara, Battelle Memorial Institute, completed the HBM model update from two to three input surfaces.

Conflicts of Interest: The authors declare no conflict of interest.

Disclaimer: The EPA Office of Research and Development was an active participant in this study. Although the EPA reviewed and approved the final manuscript for

publication, the content of this paper, nor the conclusions reached by the authors, may not necessarily reflect the official Agency policy. Mention of trade names or commercial products in this manuscript does not constitute endorsement or recommendation for use by the EPA or the authors.

References

1. Amsalu, E.; Wang, T.; Li, H.; Liu, Y.; Wang, A.; Liu, X.; Tao, L.; Luo, Y.; Zhang, F.; Yang, X.; Li, X.; Wang, W.; Guo, X., Acute effects of fine particulate matter (PM2.5) on hospital admissions for cardiovascular disease in Beijing, China: a time-series study. *Environmental health: a global access science source* **2019,** 18, (1), 70.
2. Argacha, J. F.; Collart, P.; Wauters, A.; Kayaert, P.; Lochy, S.; Schoors, D.; Sonck, J.; de Vos, T.; Forton, M.; Brasseur, O.; Beauloye, C.; Gevaert, S.; Evrard, P.; Coppieters, Y.; Sinnaeve, P.; Claeys, M. J., Air pollution and ST-elevation myocardial infarction: A case-crossover study of the Belgian STEMI registry 2009-2013. *International journal of cardiology* **2016,** 223, 300-305.
3. Braggio, J. T.; Hall, E. S.; Weber, S. A.; Huff, A. K., Contribution of Satellite-Derived Aerosol Optical Depth PM2.5 Bayesian Concentration Surfaces to Respiratory-Cardiovascular Chronic Disease Hospitalizations in Baltimore, Maryland. *Atmosphere (Basel)* **2020,** 11, (2), 209.
4. Brook, R. D.; Kousha, T., Air Pollution and Emergency Department Visits for Hypertension in Edmonton and Calgary, Canada: A Case-Crossover Study. *Am J Hypertens* **2015,** 28, (9), 1121-6.
5. Burgan, O.; Smargiassi, A.; Perron, S.; Kosatsky, T., Cardiovascular effects of sub-daily levels of ambient fine particles: a systematic review. *Environmental health: a global access science source* **2010,** 9, 26.
6. Butland, B. K.; Anderson, H. R.; van Donkelaar, A.; Fuertes, E.; Brauer, M.; Brunekreef, B.; Martin, R. V.; the, I. P. T. S. G., Ambient air pollution and the prevalence of rhinoconjunctivitis in adolescents: a worldwide ecological analysis. *Air Quality, Atmosphere & Health* **2018,** 11, (7), 755-764.
7. Chen, K.; Glonek, G.; Hansen, A.; Williams, S.; Tuke, J.; Salter, A.; Bi, P., The effects of air pollution on asthma hospital admissions in Adelaide, South Australia, 2003-2013: time-series and case-crossover analyses. *Clin Exp Allergy* **2016,** 46, (11), 1416-1430.
8. Cheng, M. H.; Chen, C. C.; Chiu, H. F.; Yang, C. Y., Fine particulate air pollution and hospital admissions for asthma: a case-crossover study in Taipei. *J Toxicol Environ Health A* **2014,** 77, (18), 1075-83.
9. Davila Cordova, J. E.; Tapia Aguirre, V.; Vasquez Apestegui, V.; Ordoñez Ibarguen, L.; Vu, B. N.; Steenland, K.; Gonzales, G. F., Association of PM(2.5) concentration with health center outpatient visits for respiratory diseases of children under 5 years old in Lima, Peru. *Environmental health: a global access science source* **2020,** 19, (1), 7.
10. Goldberg, M. S.; Burnett, R. T.; Stieb, D. M.; Brophy, J. M.; Daskalopoulou, S. S.; Valois, M. F.; Brook, J. R., Associations between ambient air pollution and daily mortality among elderly persons in Montreal, Quebec. *The Science of the total environment* **2013,** 463-464, 931-42.
11. Greene, N. A.; Morris, V. R., Assessment of public health risks associated with atmospheric exposure to PM2.5 in Washington, DC, USA. *International journal of environmental research and public health* **2006,** 3, (1), 86-97.
12. Hoek, G.; Krishnan, R. M.; Beelen, R.; Peters, A.; Ostro, B.; Brunekreef, B.; Kaufman, J. D., Long-term air pollution exposure and cardio- respiratory mortality: a review. *Environmental health: a global access science source* **2013,** 12, (1), 43.
13. Khalili, R.; Bartell, S. M.; Hu, X.; Liu, Y.; Chang, H. H.; Belanoff, C.; Strickland, M. J.; Vieira, V. M., Early-life exposure to PM2.5 and risk of acute asthma clinical encounters among children in Massachusetts: a case-crossover analysis. *Environmental health: a global access science source* **2018,** 17, (1), 20.
14. Kloog, I.; Coull, B. A.; Zanobetti, A.; Koutrakis, P.; Schwartz, J. D., Acute and chronic effects of particles on hospital admissions in New-England. *PLoS One* **2012,** 7, (4), e34664.
15. Kloog, I.; Ridgway, B.; Koutrakis, P.; Coull, B. A.; Schwartz, J. D., Long- and short-term exposure to PM2.5 and mortality: using novel exposure models. *Epidemiology (Cambridge, Mass.)* **2013,** 24, (4), 555-61.
16. Lee, M.; Koutrakis, P.; Coull, B.; Kloog, I.; Schwartz, J., Acute effect of fine particulate matter on mortality in three Southeastern states from 2007-2011. *J Expo Sci Environ Epidemiol* **2016,** 26, (2), 173-9.
17. Li, M.; Wu, Y.; Tian, Y. H.; Cao, Y. Y.; Song, J.; Huang, Z.; Wang, X. W.; Hu, Y. H., Association Between PM2.5 and Daily Hospital Admissions for Heart Failure: A Time-Series Analysis in Beijing. *International journal of environmental research and public health* **2018,** 15, (10).
18. Lim, H.; Kwon, H. J.; Lim, J. A.; Choi, J. H.; Ha, M.; Hwang, S. S.; Choi, W. J., Short-term Effect of Fine Particulate Matter on Children's Hospital Admissions and Emergency Department Visits for Asthma: A Systematic Review and Meta-analysis. *J Prev Med Public Health* **2016,** 49, (4), 205-19.
19. Liu, H.; Tian, Y.; Song, J.; Cao, Y.; Xiang, X.; Huang, C.; Li, M.; Hu, Y., Effect of Ambient Air Pollution on Hospitalization for Heart Failure in 26 of China's Largest Cities. *Am J Cardiol* **2018,** 121, (5), 628-633.
20. Liu, C.-J.; Liu, C.-Y.; Mong, N. T.; Chou, C. C. K., Spatial Correlation of Satellite-Derived PM2.5 with Hospital Admissions for Respiratory Diseases. *Remote Sensing* **2016,** 8, (11), 914.

21. Luo, L.; Zhang, Y.; Jiang, J.; Luan, H.; Yu, C.; Nan, P.; Luo, B.; You, M., Short-Term Effects of Ambient Air Pollution on Hospitalization for Respiratory Disease in Taiyuan, China: A Time-Series Analysis. *International journal of environmental research and public health* **2018,** 15, (10).
22. Mao, M.; Zhang, X.; Shao, Y.; Yin, Y., Spatiotemporal Variations and Factors of Air Quality in Urban Central China during 2013-2015. *International journal of environmental research and public health* **2019,** 17, (1).
23. Miller, L.; Xu, X., Ambient PM2.5 Human Health Effects—Findings in China and Research Directions. *Atmosphere* **2018,** 9, (11), 424.
24. Pinault, L.; Tjepkema, M.; Crouse, D. L.; Weichenthal, S.; van Donkelaar, A.; Martin, R. V.; Brauer, M.; Chen, H.; Burnett, R. T., Risk estimates of mortality attributed to low concentrations of ambient fine particulate matter in the Canadian community health survey cohort. *Environmental health: a global access science source* **2016,** 15, 18.
25. Pruss-Ustun, A.; van Deventer, E.; Mudu, P.; Campbell-Lendrum, D.; Vickers, C.; Ivanov, I.; Forastiere, F.; Gumy, S.; Dora, C.; Adair-Rohani, H.; Neira, M., Environmental risks, and non-communicable diseases. *BMJ* **2019,** 364, l265.
26. Rich, D. Q.; Utell, M. J.; Croft, D. P.; Thurston, S. W.; Thevenet-Morrison, K.; Evans, K. A.; Ling, F. S.; Tian, Y.; Hopke, P. K., Daily land use regression estimated woodsmoke and traffic pollution concentrations and the triggering of ST-elevation myocardial infarction: a case-crossover study. *Air Quality, Atmosphere & Health* **2018,** 11, (2), 239-244.
27. Shah, A. S.; Langrish, J. P.; Nair, H.; McAllister, D. A.; Hunter, A. L.; Donaldson, K.; Newby, D. E.; Mills, N. L., Global association of air pollution and heart failure: a systematic review and meta-analysis. *Lancet* **2013,** 382, (9897), 1039-48.
28. Shin, J.; Oh, J.; Kang, I. S.; Ha, E.; Pyun, W. B., Effect of Short-Term Exposure to Fine Particulate Matter and Temperature on Acute Myocardial Infarction in Korea. *International journal of environmental research and public health* **2021,** 18, (9).
29. Strosnider, H. M.; Chang, H. H.; Darrow, L. A.; Liu, Y.; Vaidyanathan, A.; Strickland, M. J., Age-Specific Associations of Ozone and Fine Particulate Matter with Respiratory Emergency Department Visits in the United States. *American journal of respiratory and critical care medicine* **2019,** 199, (7), 882-890.
30. Tapia, V.; Steenland, K.; Sarnat, S. E.; Vu, B.; Liu, Y.; Sanchez-Ccoyllo, O.; Vasquez, V.; Gonzales, G. F., Time-series analysis of ambient PM2.5 and cardiorespiratory emergency room visits in Lima, Peru during 2010-2016. *J Expo Sci Environ Epidemiol* **2020,** 30, (4), 680-688.
31. Wang, C.; Feng, L.; Chen, K., The impact of ambient particulate matter on hospital outpatient visits for respiratory and circulatory system disease in an urban Chinese population. *The Science of the total environment* **2019,** 666, 672-679.
32. Weber, S. A.; Insaf, T. Z.; Hall, E. S.; Talbot, T. O.; Huff, A. K., Assessing the impact of fine particulate matter (PM2.5) on respiratory-cardiovascular chronic diseases in the New York City Metropolitan area using Hierarchical Bayesian Model estimates. *Environ Res* **2016,** 151, 399-409.
33. Xia, X.; Yao, L., Spatio-Temporal Differences in Health Effect of Ambient PM2.5 Pollution on Acute Respiratory Infection Between Children and Adults. *IEEE Access* **2019,** 7, 25718-25726.
34. Yuan, S.; Wang, J.; Jiang, Q.; He, Z.; Huang, Y.; Li, Z.; Cai, L.; Cao, S., Long-term exposure to PM2.5 and stroke: A systematic review and meta-analysis of cohort studies. *Environ Res* **2019,** 177, 108587.
35. Babin, S. M.; Burkom, H. S.; Holtry, R. S.; Tabernero, N. R.; Stokes, L. D.; Davies-Cole, J. O.; DeHaan, K.; Lee, D. H., Pediatric patient asthma-related emergency department visits and admissions in Washington, DC, from 2001-2004, and associations with air quality, socio-economic status, and age group. *Environmental health: a global access science source* **2007,** 6, 9.
36. Babin, S.; Burkom, H.; Holtry, R.; Tabernero, N.; Davies-Cole, J.; Stokes, L.; Dehaan, K.; Lee, D., Medicaid patient asthma-related acute care visits and their associations with ozone and particulates in Washington, DC, from 1994-2005. *International journal of environmental health research* **2008,** 18, (3), 209-21.
37. Clements, A.; Herrera, R.; Hurn, S., Network analysis: a novel approach to identify PM2.5 hotspots and their spatio-temporal impact on air quality in Santiago de Chile. *Air Quality, Atmosphere & Health* **2020,** 13, (9), 1075-1082.
38. EPA (U.S. Environmental Protection Agency) (2021) Air Quality System (AQS). https://www.epa.gov/aqs. Accessed on 14 November 2021.
39. Haley, V. B.; Talbot, T. O.; Felton, H. D., Surveillance of the short-term impact of fine particle air pollution on cardiovascular disease hospitalizations in New York State. *Environmental health: a global access science source* **2009,** 8, 42.
40. Hirshon, J. M.; Shardell, M.; Alles, S.; Powell, J. L.; Squibb, K.; Ondov, J.; Blaisdell, C. J., Elevated ambient air zinc increases pediatric asthma morbidity. *Environmental health perspectives* **2008,** 116, (6), 826-31.
41. Rodopoulou, S.; Samoli, E.; Chalbot, M. G.; Kavouras, I. G., Air pollution and cardiovascular and respiratory emergency visits in Central Arkansas: A time-series analysis. *The Science of the total environment* **2015,** 536, 872-879.
42. Symons, J. M.; Wang, L.; Guallar, E.; Howell, E.; Dominici, F.; Schwab, M.; Ange, B. A.; Samet, J.; Ondov, J.; Harrison, D.; Geyh, A., A case-crossover study of fine particulate matter air pollution and onset of congestive heart failure symptom exacerbation leading to hospitalization. *Am J Epidemiol* **2006,** 164, (5), 421-33.
43. Bell, M. L.; Ebisu, K., Environmental inequality in exposures to airborne particulate matter components in the United States. *Environmental health perspectives* **2012,** 120, (12), 1699-704.
44. Brochu, P. J.; Yanosky, J. D.; Paciorek, C. J.; Schwartz, J.; Chen, J. T.; Herrick, R. F.; Suh, H. H., Particulate air pollution and socioeconomic position in rural and urban areas of the Northeastern United States. *American journal of public health* **2011,** 101 Suppl 1, (S1), S224-30.
45. Brook, R. D.; Bard, R. L.; Morishita, M.; Dvonch, J. T.; Wang, L.; Yang, H. Y.; Spino, C.; Mukherjee, B.; Kaplan, M. J.; Yalavarthi, S.; Oral, E. A.; Ajluni, N.; Sun, Q.; Brook, J. R.; Harkema, J.; Rajagopalan, S., Hemodynamic, autonomic, and vascular

effects of exposure to coarse particulate matter air pollution from a rural location. *Environmental health perspectives* **2014,** 122, (6), 624-30.
46. Fu, D.; Song, Z.; Zhang, X.; Wu, Y.; Duan, M.; Pu, W.; Ma, Z.; Quan, W.; Zhou, H.; Che, H.; Xia, X., Similarities and Differences in the Temporal Variability of PM2.5 and AOD Between Urban and Rural Stations in Beijing. *Remote Sensing* **2020,** 12, (7), 1193.
47. Han, W.; Li, Z.; Guo, J.; Su, T.; Chen, T.; Wei, J.; Cribb, M., The Urban–Rural Heterogeneity of Air Pollution in 35 Metropolitan Regions across China. *Remote Sensing* **2020,** 12, (14), 2320.
48. Lee, M.; Kloog, I.; Chudnovsky, A.; Lyapustin, A.; Wang, Y.; Melly, S.; Coull, B.; Koutrakis, P.; Schwartz, J., Spatiotemporal prediction of fine particulate matter using high-resolution satellite images in the Southeastern US 2003-2011. *J Expo Sci Environ Epidemiol* **2016,** 26, (4), 377-84.
49. Ross, Z.; Ito, K.; Johnson, S.; Yee, M.; Pezeshki, G.; Clougherty, J. E.; Savitz, D.; Matte, T., Spatial and temporal estimation of air pollutants in New York City: exposure assignment for use in a birth outcomes study. *Environmental health: a global access science source* **2013,** 12, 51.
50. Chao, C.-Y.; Zhang, H.; Hammer, M.; Zhan, Y.; Kenney, D.; Martin, R. V.; Biswas, P., Integrating Fixed Monitoring Systems with Low-Cost Sensors to Create High-Resolution Air Quality Maps for the Northern China Plain Region. *ACS Earth and Space Chemistry* **2021**.
51. Luong, N. D.; Hieu, B. T.; Hiep, N. H., Contrasting seasonal pattern between ground-based PM2.5 and MODIS satellite-based aerosol optical depth (AOD) at an urban site in Hanoi, Vietnam. *Environmental science and pollution research international* **2021**.
52. Sowden, M.; Blake, D., Using infrared geostationary remote sensing to determine particulate matter ground-level composition and concentration. *Air Quality, Atmosphere & Health* **2021**.
53. Belle, J. H.; Liu, Y., Evaluation of Aqua MODIS Collection 6 AOD Parameters for Air Quality Research over the Continental United States. *Remote Sensing* **2016,** 8, (10), 815.
54. Chang, H. H.; Hu, X.; Liu, Y., Calibrating MODIS aerosol optical depth for predicting daily PM2.5 concentrations via statistical downscaling. *J Expo Sci Environ Epidemiol* **2014,** 24, (4), 398-404.
55. Cheng, L.; Li, L.; Chen, L.; Hu, S.; Yuan, L.; Liu, Y.; Cui, Y.; Zhang, T., Spatiotemporal Variability, and Influencing Factors of Aerosol Optical Depth over the Pan Yangtze River Delta during the 2014-2017 Period. *International journal of environmental research and public health* **2019,** 16, (19).
56. Christopher, S.; Gupta, P., Global Distribution of Column Satellite Aerosol Optical Depth to Surface PM2.5 Relationships. *Remote Sensing* **2020,** 12, (12), 1985.
57. He, Q.; Zhang, M.; Huang, B., Spatio-temporal variation, and impact factors analysis of satellite-based aerosol optical depth over China from 2002 to 2015. *Atmospheric Environment* **2016,** 129, 79-90.
58. He, Q.; Gu, Y.; Zhang, M., Spatiotemporal patterns of aerosol optical depth throughout China from 2003 to 2016. *The Science of the total environment* **2019,** 653, 23-35.
59. Hu, Z., Spatial analysis of MODIS aerosol optical depth, PM2.5, and chronic coronary heart disease. *Int J Health Geogr* **2009,** 8, 27.
60. Hu, Z.; Rao, K. R., Particulate air pollution and chronic ischemic heart disease in the eastern United States: a county level ecological study using satellite aerosol data. *Environmental health: a global access science source* **2009,** 8, 26.
61. Hu, X.; Waller, L. A.; Lyapustin, A.; Wang, Y.; Liu, Y., 10-year spatial and temporal trends of PM2.5 concentrations in the southeastern US estimated using high-resolution satellite data. *Atmos Chem Phys* **2014,** 14, (12), 6301-6314.
62. Kumar, N.; Chu, A.; Foster, A., An empirical relationship between PM(2.5) and aerosol optical depth in Delhi Metropolitan. *Atmos Environ (1994)* **2007,** 41, (21), 4492-4503.
63. Kumar, N.; Chu, A. D.; Foster, A. D.; Peters, T.; Willis, R., Satellite Remote Sensing for Developing Time, and Space Resolved Estimates of Ambient Particulate in Cleveland, OH. *Aerosol Sci Technol* **2011,** 45, (9), 1090-1108.
64. Kumar, N.; Liang, D.; Comellas, A.; Chu, A. D.; Abrams, T., Satellite-based PM concentrations and their application to COPD in Cleveland, OH. *J Expo Sci Environ Epidemiol* **2013,** 23, (6), 637-46.
65. Lee, D.; Byun, D. W.; Kim, H.; Ngan, F.; Kim, S.; Lee, C.; Cho, C., Improved CMAQ predictions of particulate matter utilizing the satellite-derived aerosol optical depth. *Atmospheric Environment* **2011,** 45, (22), 3730-3741.
66. Lee, H. J.; Coull, B. A.; Bell, M. L.; Koutrakis, P., Use of satellite-based aerosol optical depth and spatial clustering to predict ambient PM2.5 concentrations. *Environ Res* **2012,** 118, 8-15.
67. Li, J.; Carlson, B. E.; Lacis, A. A., How well do satellite AOD observations represent the spatial and temporal variability of PM 2.5 concentration for the United States? *Atmospheric Environment* **2015,** 102, 260-273.
68. Li, Y.; Henze, D. K.; Jack, D.; Kinney, P. L., The influence of air quality model resolution on health impact assessment for fine particulate matter and its components. *Air Quality, Atmosphere & Health* **2016,** 9, (1), 51-68.
69. Lien, W. H.; Owili, P. O.; Muga, M. A.; Lin, T. H., Ambient Particulate Matter Exposure and Under-Five and Maternal Deaths in Asia. *International journal of environmental research and public health* **2019,** 16, (20).
70. Long, Y.; Wang, J.; Wu, K.; Zhang, J., Population Exposure to Ambient PM2.5 at the Subdistrict Level in China. *International journal of environmental research and public health* **2018,** 15, (12).

71. Mirzaei, M.; Bertazzon, S.; Couloigner, I.; Farjad, B.; Ngom, R., Estimation of local daily PM2.5 concentration during wildfire episodes: integrating MODIS AOD with multivariate linear mixed effect (LME) models. *Air Quality, Atmosphere & Health* **2020,** 13, (2), 173-185.
72. Owili, P. O.; Lien, W. H.; Muga, M. A.; Lin, T. H., The Associations between Types of Ambient PM2.5 and Under-Five and Maternal Mortality in Africa. *International journal of environmental research and public health* **2017,** 14, (4).
73. Sorek-Hamer, M.; Just, A. C.; Kloog, I., Satellite remote sensing in epidemiological studies. *Curr Opin Pediatr* **2016,** 28, (2), 228-34.
74. Tamayo-Ortiz, M.; Tellez-Rojo, M. M.; Rothenberg, S. J.; Gutierrez-Avila, I.; Just, A. C.; Kloog, I.; Texcalac-Sangrador, J. L.; Romero-Martinez, M.; Bautista-Arredondo, L. F.; Schwartz, J.; Wright, R. O.; Riojas-Rodriguez, H., Exposure to PM2.5 and Obesity Prevalence in the Greater Mexico City Area. *International journal of environmental research and public health* **2021,** 18, (5).
75. Viana, J.; Santos, J. V.; Neiva, R. M.; Souza, J.; Duarte, L.; Teodoro, A. C.; Freitas, A., Remote Sensing in Human Health: A 10-Year Bibliometric Analysis. *Remote Sensing* **2017,** 9, (12), 1225.
76. Vu, B. N.; Sanchez, O.; Bi, J.; Xiao, Q.; Hansel, N. N.; Checkley, W.; Gonzales, G. F.; Steenland, K.; Liu, Y., Developing an Advanced PM2.5 Exposure Model in Lima, Peru. *Remote Sens (Basel)* **2019,** 11, (6).
77. Wang, Y.; Hu, X.; Chang, H. H.; Waller, L. A.; Belle, J. H.; Liu, Y., A Bayesian Downscaler Model to Estimate Daily PM2.5 Levels in the Conterminous US. *International journal of environmental research and public health* **2018,** 15, (9).
78. Xue, T.; Zheng, Y.; Geng, G.; Zheng, B.; Jiang, X.; Zhang, Q.; He, K., Fusing Observational, Satellite Remote Sensing and Air Quality Model Simulated Data to Estimate Spatiotemporal Variations of PM2.5 Exposure in China. *Remote Sensing* **2017,** 9, (3), 221.
79. Geng, G.; Murray, N. L.; Chang, H. H.; Liu, Y., The sensitivity of satellite-based PM2.5 estimates to its inputs: Implications to model development in data-poor regions. *Environment international* **2018,** 121, (Pt 1), 550-560.
80. Kloog, I.; Chudnovsky, A. A.; Just, A. C.; Nordio, F.; Koutrakis, P.; Coull, B. A.; Lyapustin, A.; Wang, Y.; Schwartz, J., A New Hybrid Spatio-Temporal Model For Estimating Daily Multi-Year PM2.5 Concentrations Across Northeastern USA Using High Resolution Aerosol Optical Depth Data. *Atmos Environ (1994)* **2014,** 95, 581-590.
81. Liu, Y.; Paciorek, C. J.; Koutrakis, P., Estimating regional spatial and temporal variability of PM(2.5) concentrations using satellite data, meteorology, and land use information. *Environmental health perspectives* **2009,** 117, (6), 886-92.
82. McGuinn, L. A.; Ward-Caviness, C. K.; Neas, L. M.; Schneider, A.; Diaz-Sanchez, D.; Cascio, W. E.; Kraus, W. E.; Hauser, E.; Dowdy, E.; Haynes, C.; Chudnovsky, A.; Koutrakis, P.; Devlin, R. B., Association between satellite-based estimates of long-term PM2.5 exposure and coronary artery disease. *Environ Res* **2016,** 145, 9-17.
83. EPA (U.S. Environmental Protection Agency) The Community Modeling and Analysis System, CMAQ. https:/www.epa.gocv/cmaq. Accessed on 14 November 2021.
84. Braggio, J. T.; Hall, E. S.; Weber, S. A.; Huff, A. K., Contribution of AOD-PM2.5 surfaces to respiratory-cardiovascular hospital events in urban and rural areas in Baltimore, Maryland, USA: New analytical method correctly identified true positive cases and true negative controls. *Atmospheric Environment* **2021,** 262, 118629.
85. Batterman, S.; Xu, L.; Chen, F.; Chen, F.; Zhong, X., Characteristics of PM2.5 Concentrations across Beijing during 2013-2015. *Atmos Environ (1994)* **2016,** 145, 104-114.
86. Dabass, A.; Talbott, E. O.; Bilonick, R. A.; Rager, J. R.; Venkat, A.; Marsh, G. M.; Duan, C.; Xue, T., Using spatio-temporal modeling for exposure assessment in an investigation of fine particulate air pollution and cardiovascular mortality. *Environ Res* **2016,** 151, 564-572.
87. Erickson, A. C.; Ostry, A.; Chan, L. H.; Arbour, L., The reduction of birth weight by fine particulate matter and its modification by maternal and neighbourhood-level factors: a multilevel analysis in British Columbia, Canada. *Environmental health: a global access science source* **2016,** 15, 51.
88. Yanosky, J. D.; Paciorek, C. J.; Laden, F.; Hart, J. E.; Puett, R. C.; Liao, D.; Suh, H. H., Spatio-temporal modeling of particulate air pollution in the conterminous United States using geographic and meteorological predictors. *Environmental health: a global access science source* **2014,** 13, 63.
89. Cai, K.; Zhang, Q.; Li, S.; Li, Y.; Ge, W., Spatial(-)Temporal Variations in NO(2) and PM2.5 over the Chengdu(-)Chongqing Economic Zone in China during 2005(-)2015 Based on Satellite Remote Sensing. *Sensors (Basel)* **2018,** 18, (11).
90. Coker, E.; Ghosh, J.; Jerrett, M.; Gomez-Rubio, V.; Beckerman, B.; Cockburn, M.; Liverani, S.; Su, J.; Li, A.; Kile, M. L.; Ritz, B.; Molitor, J., Modeling spatial effects of PM(2.5) on term low birth weight in Los Angeles County. *Environ Res* **2015,** 142, 354-64.
91. Huang, C.; Liu, K.; Zhou, L., Spatio-temporal trends and influencing factors of PM2.5 concentrations in urban agglomerations in China between 2000 and 2016. *Environmental science and pollution research international* **2021,** 28, (9), 10988-11000.
92. Liu, Y., New Directions: Satellite driven PM2.5 exposure models to support targeted particle pollution health effects research. *Atmospheric Environment* **2013,** 68, 52-53.
93. Zeng, M.; Du, J.; Zhang, W., Spatial-Temporal Effects of PM2.5 on Health Burden: Evidence from China. *International journal of environmental research and public health* **2019,** 16, (23).
94. Hall ES (2018). Temporal-Spatial Ambient Concentrator Estimator (T-SpACE): Hierarchical Bayesian Model Software Used to Estimate Ambient Concentrations of NAAQS Air Pollutants in Support of Health Studies. United States Environmental Protection Agency, Washington, DC, EPA/600/R-18/01, 2018. https://cfpub.epa.gov/si/si_public_record_report.cfm?Lab=NERL&dirEntryId=339714. Accessed on 14 November 2021.

95. McMillan, N. J.; Holland, D. M.; Morara, M.; Feng, J., Combining numerical model output and particulate data using Bayesian space-time modeling. *Environmetrics* **2009,** 21, (1), n/a-n/a.
96. Weber, S. A.; Engel-Cox, J. A.; Hoff, R. M.; Prados, A. I.; Zhang, H., An improved method for estimating surface fine particle concentrations using seasonally adjusted satellite aerosol optical depth. *Journal of the Air & Waste Management Association (1995)* **2010,** 60, (5), 574-85.
97. Bell, M. L.; Ebisu, K.; Peng, R. D.; Walker, J.; Samet, J. M.; Zeger, S. L.; Dominici, F., Seasonal and regional short-term effects of fine particles on hospital admissions in 202 US counties, 1999-2005. *Am J Epidemiol* **2008,** 168, (11), 1301-10.
98. Hsu, W. H.; Hwang, S. A.; Kinney, P. L.; Lin, S., Seasonal and temperature modifications of the association between fine particulate air pollution and cardiovascular hospitalization in New York state. *The Science of the total environment* **2017,** 578, 626-632.
99. Liu, X.; Bertazzon, S., Exploratory Temporal and Spatial Analysis of Myocardial Infarction Hospitalizations in Calgary, Canada. *International journal of environmental research and public health* **2017,** 14, (12).
100. HSCRC (Maryland Health Services Cost Review Commission), ED and IP data, 2004-2006. https://hscrc.state.md.us/pages/default.aspx. Accessed on 14 November 2021.
101. USPS (U. S. Postal Service Office of Inspector General), "The untold story of the ZIP Code," April 1, 013, RARC-WP-13-006. https://permanent.fdlp.gov/gpo47009/rarc-wp-13-006.pdf. Accessed on 14 November 2021.
102. CDC (U.S. Centers for Disease Control and Prevention), National Center for Health Statistics (NCHS), International Classification of Diseases, Ninth Revision, Clinical Modification (ICD-9-CM), 2011. https://www.cdc.gov/nchs/icd/icd9cm.htm. Accessed on 14 November 2021.
103. MDH (Maryland Department of Health), Institutional Review Board. https://health.maryland.gov/oig/irb/Pages/IRB.aspx. Accessed on 14 November 2021.
104. Maclure, M., The case-crossover design: a method for studying transient effects on the risk of acute events. *Am J Epidemiol* **1991,** 133, (2), 144-53.
105. Carracedo-Martinez, E.; Taracido, M.; Tobias, A.; Saez, M.; Figueiras, A., Case-crossover analysis of air pollution health effects: a systematic review of methodology and application. *Environmental health perspectives* **2010,** 118, (8), 1173-82.
106. Dzhambov, A. M.; Dimitrova, D. D., Exposures to road traffic, noise, and air pollution as risk factors for type 2 diabetes: A feasibility study in Bulgaria. *Noise & health* **2016,** 18, (82), 133-42.
107. Hansen, A. B.; Ravnskjaer, L.; Loft, S.; Andersen, K. K.; Brauner, E. V.; Baastrup, R.; Yao, C.; Ketzel, M.; Becker, T.; Brandt, J.; Hertel, O.; Andersen, Z. J., Long-term exposure to fine particulate matter and incidence of diabetes in the Danish Nurse Cohort. *Environment international* **2016,** 91, 243-50.
108. Weinmayr, G.; Hennig, F.; Fuks, K.; Nonnemacher, M.; Jakobs, H.; Mohlenkamp, S.; Erbel, R.; Jockel, K. H.; Hoffmann, B.; Moebus, S.; Heinz Nixdorf Recall Investigator, G., Long-term exposure to fine particulate matter and incidence of type 2 diabetes mellitus in a cohort study: effects of total and traffic-specific air pollution. *Environmental health: a global access science source* **2015,** 14, 53.
109. NOAA (National Oceanic and Atmospheric Administration), The New Improved "Wind Chill Index." https://www.weather.gov/ffc/wci. Accessed on 14 November 2021.
110. Rothfusz LP (1990) The Heat Index "Equation," SR-90-23, 7/1/90. https://www.weather.gov/media/ffc/ta_htindx.PDF. Accessed on 14 November 2021.
111. Braggio J.T.; Brunner W.; Lutzker L.; Managan A.; Simms E.; Tomasallo C.; Wahl, R.; Yip, F. *Analysis of 2009 pollen readings in Atlanta, GA, Baltimore, MD, and Madison, WI.* Proceedings of the Council of State and Territorial Epidemiologists Conference, Omaha, NE, June 4-7, 2012. https://cdn.ymaws.com/www.cste.org/resource/resmgr/EnvironmentalHealth/AYip-PollenAtlantaBaltimoreMa.pdf. Accessed on 14 November 2021.
112. Guilbert, A.; Cox, B.; Bruffaerts, N.; Hoebeke, L.; Packeu, A.; Hendrickx, M.; De Cremer, K.; Bladt, S.; Brasseur, O.; Van Nieuwenhuyse, A., Relationships between aeroallergen levels and hospital admissions for asthma in the Brussels-Capital Region: a daily time series analysis. *Environmental health: a global access science source* **2018,** 17, (1), 35.
113. Ito, K.; Weinberger, K. R.; Robinson, G. S.; Sheffield, P. E.; Lall, R.; Mathes, R.; Ross, Z.; Kinney, P. L.; Matte, T. D., The associations between daily spring pollen counts, over-the-counter allergy medication sales, and asthma syndrome emergency department visits in New York City, 2002-2012. *Environmental health: a global access science source* **2015,** 14, 71.
114. Weichenthal, S.; Lavigne, E.; Villeneuve, P. J.; Reeves, F., Airborne Pollen Concentrations and Emergency Room Visits for Myocardial Infarction: A Multicity Case-Crossover Study in Ontario, Canada. *Am J Epidemiol* **2016,** 183, (7), 613-21.
115. Wu H.C.; Saptoka A.; Braggio J.T. *Pollen effects on asthma, allergic rhinitis, and finger wound emergency department visits between 2000-2010 in Baltimore, Maryland.* Proceedings of the Council of State and Territorial Epidemiologists Conference, Nashville, TN, June 22-26, 2014. https://phpa.health.maryland.gov/OEHFP/EH/Climate%20Change%20Binder/8-CSTE_2014_Pollen-Asthma_Poster.pdf. Accessed on 14 November 2021.
116. OPM (Office of Personnel Management), Federal Holidays, 2004-2006. https://archive.opm.gov/Operating_Status_Schedules/fedhol/2004.asp. Accessed on 14 November 2021.
117. NCEI (National Centers for Environmental Information, National Oceanic and Atmospheric Adeministration), Online Climate Data. https://www.ncdc.noaa.gov/cdo-web/. Accessed on 14 November 2021.

118. Newell, K.; Kartsonaki, C.; Lam, K. B. H.; Kurmi, O. P., Cardiorespiratory health effects of particulate ambient air pollution exposure in low-income and middle-income countries: a systematic review and meta-analysis. *Lancet Planet Health* **2017,** 1, (9), e368-e380.
119. O'Lenick, C. R.; Winquist, A.; Mulholland, J. A.; Friberg, M. D.; Chang, H. H.; Kramer, M. R.; Darrow, L. A.; Sarnat, S. E., Assessment of neighbourhood-level socioeconomic status as a modifier of air pollution-asthma associations among children in Atlanta. *J Epidemiol Community Health* **2017,** 71, (2), 129-136.
120. Wilson, W. E.; Mar, T. F.; Koenig, J. Q., Influence of exposure error and effect modification by socioeconomic status on the association of acute cardiovascular mortality with particulate matter in Phoenix. *J Expo Sci Environ Epidemiol* **2007,** 17 Suppl 2, S11-9.
121. USCB (U.S. Census Bureau), Census of People and Housing, Summary File 3. https://www.census.gov/data/datasets/2000/dec/summary-file-3.html. Accessed on 14 November 2021.
122. MDP (Maryland Department of Planning), Maryland State Date Center, Zip code boundary area files, 2004 and 2006. http://planning.maryland.gov/MSDC/Pages/s5_map_gis.aspx. Accessed on 14 November 2021.
123. Braggio J.T.; Weber S.; Young E.; Hall E. *Contribution of hierarchical Bayesian and aerosol optical depth $PM_{2.5}$ sources to respiratory-cardiovascular chronic diseases.* Proceedings of the International Society for Environmental Epidemiology Conference, Seattle, WA, August 24-28, 2014. Abstract published in *Environmental Health Perspectives*, Vol. 2014, p 1899. https://www.researchgate.net/publication/337517983_Contribution_of_Hierarchical_Bayesian_and_Aerosol_Optical_Depth_PM_25_Sources_to_Respiratory-Cardiovascular_Chronic_Diseases. Accessed on 14 November 2021.
124. ESRI (Environmental Systems Research Institute). *ArcGIS Desktop (ArcMap)* Release 10.6.1. Redlands, CA, 2018,
125. Agresti, A., *Categorical Data Analysis*. John Wiley & Sons: Hoboken, New Jersey, 2002.
126. Hosmer DW, J., Lemeshow S, Sturdivant RX *Applied Logistic Regression*. 3rd ed.; John Wiley & Sons: Hoboken, NJ, 2013.
127. SAS (Statistical Analysis System). *Base SAS 9.4 (7th Ed)*. SAS Institute Inc, Cary, NC, USA, 2017.
128. SAS (Statistical Analysis System). *SAS/STAT 14.1 User's Guide: High-Performance Procedures.* SAS Institute Inc, Cary, 2018.
129. Stokes M.E.; Davis C.S.; Koch G.G. *Categorical Data Analysis Using the SAS System,* 3rd ed.; SAS Institute, Inc: Cary, NC, 2012.
130. EPA (U.S. Environmental Protection Agency), Ambient Monitoring Technology Information Center (AMTIC), Baltimore PM Supersite Project Information. https://www.epa.gov/amtic/amtic-pm-supersites. Accessed on 14 November 2021.
131. EPA (U.S. Environmental Protection Agency), Toxics Release Inventory (TRI) Program. TRI Basic Data Files: Calendar Years 1987-2018. https://www.epa.gov/toxics-release-inventory-tri-program/tri-basic-data-files-calendar-years-1987-2018?.%20. Accessed on 14 November 2021.
132. Litt, J. S.; Burke, T. A., Uncovering the historic environmental hazards of urban brownfields. *J Urban Health* **2002,** 79, (4), 464-81.
133. Litt, J. S.; Tran, N. L.; Burke, T. A., Examining urban brownfields through the public health "macroscope". *Environmental health perspectives* **2002,** 110 Suppl 2, (Suppl 2), 183-93.
134. Downey, L., Environmental Inequality in Metropolitan America in 2000. *Sociol Spectr* **2006,** 26, (1), 21-41.
135. Perlin, S. A.; Sexton, K.; Wong, D. W., An examination of race and poverty for populations living near industrial sources of air pollution. *J Expo Anal Environ Epidemiol* **1999,** 9, (1), 29-48.
136. Perlin, S. A.; Wong, D.; Sexton, K., Residential proximity to industrial sources of air pollution: interrelationships among race, poverty, and age. *Journal of the Air & Waste Management Association (1995)* **2001,** 51, (3), 406-21.
137. Wilson, S.; Zhang, H.; Jiang, C.; Burwell, K.; Rehr, R.; Murray, R.; Dalemarre, L.; Naney, C., Being overburdened and medically underserved: assessment of this double disparity for populations in the state of Maryland. *Environmental health: a global access science source* **2014,** 13, (1), 26.
138. Chudnovsky, A. A.; Kostinski, A.; Lyapustin, A.; Koutrakis, P., Spatial scales of pollution from variable resolution satellite imaging. *Environmental pollution (Barking, Essex: 1987)* **2013,** 172, 131-8.
139. Harris, G.; Thompson, W. D.; Fitzgerald, E.; Wartenberg, D., The association of PM(2.5) with full term low birth weight at different spatial scales. *Environ Res* **2014,** 134, 427-34.
140. Jiang, X.; Yoo, E. H., The importance of spatial resolutions of Community Multiscale Air Quality (CMAQ) models on health impact assessment. *The Science of the total environment* **2018,** 627, 1528-1543.
141. Bowatte, G.; Lodge, C.; Lowe, A. J.; Erbas, B.; Perret, J.; Abramson, M. J.; Matheson, M.; Dharmage, S. C., The influence of childhood traffic-related air pollution exposure on asthma, allergy, and sensitization: a systematic review and a meta-analysis of birth cohort studies. *Allergy* **2015,** 70, (3), 245-56.
142. Grahame, T. J.; Schlesinger, R. B., Cardiovascular health, and particulate vehicular emissions: a critical evaluation of the evidence. *Air Quality, Atmosphere & Health* **2010,** 3, (1), 3-27.
143. Wang, B.; Chen, Z., High-resolution satellite-based analysis of ground-level PM2.5 for the city of Montreal. *The Science of the total environment* **2016,** 541, 1059-1069.